Site Directed Mutagenesis of Residue Lysine 157 of the Hypoxanthine-Guanine Phosphoribosyltransferase Gene from *Leishmania donovani*; and Kinetic Analysis and comparison of site directed mutants with the recombinant wild type enzyme.

by

Gregory Paul Barton

A Thesis

Presented to the Department of Biochemistry and
Molecular Biology
School of Medicine
Oregon Health Sciences University
in partial fulfillment of
the requirements for the degree of

Master of Science

School of Medicine
Oregon Health & Science University

CERTIFICATE OF APPROVAL

This is to certify that the Master's of Science thesis of

Gregory Barton

has been approved

[redacted]

Professor in charge of thesis – Dr. Buddy Ullman

[redacted]

Thesis Committee Chair – Dr. Richard G. Brennan

[redacted]

Thesis Committee Member – Dr. Scott Landfear

[redacted]

Thesis Committee Member – Dr. Maria A. Schumacher

Table of Contents

List of Figures

Acknowledgments

I wish to express my gratitude to the Ullman lab, where I had the opportunity to meet and work with so many wonderful people. I would like to include a special thanks to Tom Allen, who got me started and assisted me immensely when I first came into the lab. I enjoyed working with all of my colleagues and would like to specifically thank the following people for sharing their scientific knowledge with me and their friendship: Sue Bergeson, Armando Jardim, Nicola Carter, Ho Yon Hwang, John Jiang, Derrick Carter, Jerry Scott and Sarah Shih.

I would like to thank the members of my thesis advisory committee, Dick Brennan, Maria Schumacher, and Scott Landfear, who have been gracious enough to agree to sit on my committee and offer their assistance. Dick Brennan and Maria Schumacher have both been strong influences in my scientific development, as I worked with them on a joint project with the Ullman laboratory.

Dr. Buddy Ullman, as my mentor, has always been supportive of me, and I would like to especially

thank him for going to bat for me and supporting me when I asked for permission write this thesis so many years after completion of this research.

I would like to thank my wife, Karen, and my three children, Cassidy, Brittany and Forrest as well, as they have been very supportive of me and have always exhibited a great deal of understanding throughout the many years of my educational pursuits in a variety of disciplines.

Abstract

Parasitic protozoa, which are auxotrophic for purines, have evolved a unique metabolic pathway, the purine salvage pathway, to meet their requirements for purines. Since they are unable to synthesize their purines, they must salvage these essential nutrients from their hosts. Numerous enzymes are involved in allowing the parasitic protozoa to obtain the purines it needs from its host. The enzyme, hypoxanthine-guanine phosphoribosyltransferase (HGPRT) appears to be a key enzyme in purine salvage used by these parasites. This thesis examines the role of the active site residue, lysine 157, within the HGPRT of *Leishmania donovani*.

This research project started out as an attempt to crystallize the *L. donovani*, *T. cruzi*, and *T. brucei* HGPRTs for overall structural determination. After approximately two years of work, *T. cruzi* and *T. brucei* HGPRTs yielded only small rod-shaped crystals, which were unsuitable for crystallographic analysis. The *L. donovani* HGPRT was crystallized by hanging drop vapor diffusion

method; the size of the crystals was 0.4 mm by 0.2 mm, but the crystals diffracted to a maximum of 5-6 Å, which was not suitable for further crystallographic studies.

The structure of human HGPRT suggested a mechanism through which the equivalent lysine in the human enzyme to the lysine 157 in the *L. donovani* HGPRT played a key role in the specificity of the enzymes catalysis of guanine and hypoxanthine, but not adenine (43). Lysine 157 is involved in hydrogen bonding to the O6 of the purine bases hypoxanthine and guanine as determined by the crystallographic work on the human enzyme and *T. gondii* (43,45). Due to the failure of crystallographic studies, the research for this thesis was refocused to explore the role of *L. donovani* HGPRT lysine 157; five separate mutations of lysine 157 were created: alanine 157, arginine 157, methionine 157, glutamic acid 157, and glutamine 157.

Complementation studies were performed using bacterial strains lacking in phosphoribosyltransferase activities, and kinetic

studies were then undertaken showing that the K_m values for hypoxanthine and guanine for all of the mutants were raised approximately 10 to 40 fold.

Circular dichroism studies on the wild type and all five mutants were performed to show that the observed effects were not due to major structural changes in the enzyme. These studies showed that all mutated proteins were folded properly and similar to the wild-type enzyme in overall secondary structure.

INTRODUCTION

A. Parasitic Diseases

Parasites are organisms "living in or on and obtaining nourishment from another organism."(47) Protozoa and helminths comprise the two major categories of eukaryotic parasites. Parasitic organisms have a devastating effect on almost two thirds of the world's population. Developing countries pay the greatest price, both economically and in the area of public health. Malaria, caused by the parasite *Plasmodium falciparum*, is the leading killer of any disease-causing organism (1). Deaths from malaria are estimated at over one million per year (51).

Parasitic protozoa are one of the largest groups of organisms on earth with the identification of thousands of different species. Devastating parasitic diseases are most prevalent in tropical regions encompassed by developing countries; therefore, the plight of the people in these poor countries goes virtually unnoticed by the industrialized world. However, with the growth

in incidence of the AIDS virus, parasites that were previously not a problem for humans have become fatal to those infected with the AIDS virus. Therefore, developing a better understanding of these disease-causing organisms is more pressing than ever. It is estimated that it will cost $200,000,000 to develop the 20 to 30 new drugs that will be needed to effectively treat protozoan parasitic diseases (51).

Eukaryotic parasites have been a persistent problem throughout the history of medical research. The problem for the scientist is how to kill one type of eukaryote, the parasite, without killing or severely impairing the human host, another eukaryotic organism. The answer to this problem will be discovered by using the new tools available to the biochemists and molecular biologists. Through the genetic and biochemical characterization of eukaryotic parasites, biochemical pathways unique to these organisms are coming to light. Scientists are now targeting the biochemical differences between the host and the

parasite to develop new chemotherapeutic approaches to this age-old problem (53).

This thesis focuses on one of the biochemically distinct pathways found in parasitic protozoa: the purine salvage pathway. Hypoxanthine-guanine phosphoribosyltransferase (HGPRT) is one of the key enzymes within the purine salvage pathway of the parasitic protozoa. It allows the parasite to use purine bases, salvaged from the host, to synthesize the nucleotides it needs in order to thrive and replicate. Because humans can synthesize purines *de novo*, HGPRT is an ideal target for drug design. Furthermore, it has been shown that HGPRT can convert certain purine analogs to the nucleotide level; purine analogs may serve as subversive substrates, which when phophoribosylated by the parasitic HGPRT are trapped intracellularly; these trapped nucleotides may then build up to levels that are cytotoxic to the parasite.

One of the problems facing the use of purine analogs has been that at effective dosages many analogs are also toxic to the host cells (58). Even though humans hosts have the ability to *de*

novo synthesize purines, human HGPRT may phosphoribosylate purine analogs and cause cytotoxicity to the human host cells.

B. The Order Kinetoplastida

Both *Leishmania* and trypanosomes are members of the *Trypanosomatidae* family and belong to the order *Kinetoplastida*. The *Kinetoplastida*, both free living and parasitic, are comprised of flagellated organisms. Kinetoplastids have a single mitochondrion, the kinetoplast, which contains a network of thousands of interlocking DNA maxicircles and minicircles. Ninety-five percent of the DNA is made up of minicircles and the rest is in maxicircles similar to the mitochondrial DNA of other eukaryotes, which encodes the mitochondrial genes. Until recently, the role of the minicircles was not understood. Recent studies have shown that the minicircles are involved in editing the transcripts of the maxicircles to form a mature message, through a process called RNA editing (2).

The order *Kinetoplastida* is made up of two suborders: *Bodinina*, a free-living organism and

Trypanosomatina, which is exclusively parasitic. This thesis will discuss only the *Trypanosomatina*, which is made up of a single family, the *Trypanosomatidae* (Figure 1). The *Trypanosomatidae* parasites studied in this thesis are transmitted to the host through an insect vector. The life cycle of these parasites involves transmission back and forth between the insect vector and host. This back and forth transmission induces significant morphological and metabolic changes in these organisms, allowing for systematic classification of different forms of the parasites, during their life cycles (3).

C. *Trypanosoma*

The genus *Trypanosoma* is comprised of organisms, which affect both humans and other animals, as well as non-pathogenic organisms. This discussion will focus on the organisms that cause a disease state in humans. The pathogenic species are found in Africa and South America; the human diseases caused are two distinct forms: African Sleeping Sickness and Chagas disease, which is also known as South American Trypanosomiasis.

Figure 1

The Order Kinetoplastida

Kinetoplastida

Kingdom	**Protista**
Subkingdom	**Protozoa**
Phylum	**Sarcomastigophora**
Subphylum	**Mastigophora**
Class	**Zoomastigophorea**
Order	**Kinetoplastida**
Suborder	**Trypanosomatina**
Family	**Trypanosomatidae**

Genera of Family Trypanosomatidae

Trypanasoma
- Crithidia
- Herpetomonus
- Endotrypanum

Leishmania
- Leptomonas
- Phytomonas
- Rhynochoidomonas

1. South American Trypanosomiasis--Chagas Disease

South American Trypanosomiasis, *T. cruzi*, was first described by Carlos Chagas in 1909 (3). However, *T. cruzi* has been plaguing human beings for 9000 years (50). *T. cruzi* is transmitted not directly through the bite of the vector, the reduviid bug (*Reduviidae* family of arthropods), but instead through the feces, which are usually rubbed into the bite wound by the bitten human. Reservoirs of *T. cruzi* include humans, dogs, cats, rabbits, and various rodent species. *T. cruzi* afflicts mostly rural areas because the common thatch roofs or walls create an ideal environment for the reduviid bug. Furthermore, reduviid bugs are resistant to common insecticides and very resilient (3,4).

T. cruzi infection often occurs during childhood and continues for life (5,6). Chagas disease can be broken into two stages: the acute and the chronic phase. The acute phase may be very

serious in children and infants, but often asymptomatic in adults (5).

Within 4-12 days following infection, *T. cruzi* can potentially be found in any organ of the body, but often targets the heart, which can be virtually destroyed during the acute phase of the disease (7).

The chronic phase starts between the second and fourth month. Many infected individuals are asymptomatic for the rest of their lives (8). However, the leading cause of death in infected individuals is heart failure (6). Dysfunction of the central and peripheral nervous system are other symptoms, as well as enlargement of the esophagus or colon, which can lead to death.

a. Life Cycle

As previously stated, *T. cruzi* is passed through the feces of the vector through rubbing the feces into the bite wound or a mucous membrane, typically the conjunctiva of the eye. The infectious form of *T. cruzi*, the metacyclic trypomastigotes, then enter host cells, either through phagocytosis or active invasion, and change

morphology to the amastigote form (9). The amastigotes replicate, lysing the cells, and going on to invade new cells and tissue types. *T. cruzi* predominantly infects cardiac and skeletal muscle cells; and the reticuloendothelial cells of the liver and spleen (6). It has been suggested that immunologic response of the host is responsible for the observed pathology of Chagas disease (10). Various forms of the parasite exist in the host including the trypomastigote form in the bloodstream.

Trypomastigotes are taken up by the vector, migrate to the hindgut, and the environment there induces the tranformation to the vector replicative epimastigote form. The epimatigotes migrate to the rectum of the reduviid and attach themselves to the epithelium of the rectal gland. In the rectum, they transform into the infectious metacyclic trypomastigote to await their next mammalian host (3) (Figure 2).

Figure 2

T. cruzi Life Cycle

Life Cycle of South American Trypanasomes

Reduviid bug bites human host and defecates on the skin.

↓

Metacyclic trypomastigotes are rubbed into the eye or bite wound.

↓

Trypomastigotes are taken up by cells and reproduce as amastigotes.

↓

Amastigotes reproduce and lyse cell. Some amastigotes infect new cells and some transform into trypomastigotes and remain in the bloodstream.

→

Vector is infected when it takes a blood meal with trypomastigotes present.

↑

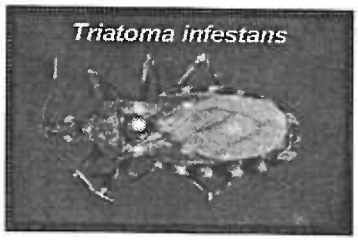

↑

Trypomastigotes migrate to the midgut where they change to epimastigote form and replicate. Then migrate to the hindgut and form metacyclic trypomastigotes

←

b. Treatment and Control of Chagas' Disease

The current treatments for Chagas' disease are woefully inadequate. The two drugs used, nifurtimox and benznidazole can successfully clear the trypomastigote form from the bloodstream, but appear to be ineffective against the amastigote form (8) (Figure 3). Both drugs often cause serious side effects involving the central nervous system and gastrointestinal tract (11). During treatment, patients test negative for the disease, but after the cessation of treatment, patients test positive again; this is indicative of the inability of the current chemotherapies to eradicate the organism once it has invaded the host cells. New drugs are desperately needed.

Control of the vector has also been unsuccessful because the *Reduviidae* family of arthropods are very resistant to all current insecticides (3,4). The rural nature of the disease also makes application of pesticides impracticable. The best approach is to change building materials and move away from the thatch construction, which harbors the vector.

Figure 3

Current Drugs used to control *T. cruzi*

The severe side effects and toxicity of these drugs often results in patients not completing treatment (54).

Drug Treatments for Chagas Disease

Nifurtimox

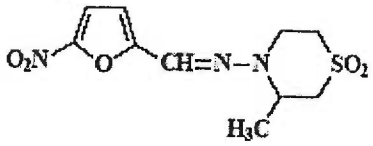

Benznidazole

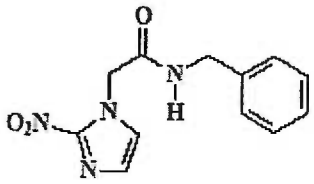

This approach has shown significant reductions in the rate of infection. However, once again, the cost of this approach makes it impracticable.

2. African Sleeping Sickness

Two subspecies of *Trypanosoma brucei*, *T.b. gambiense* and *T.b. rhodesiense*, are the causative agents of African sleeping sickness. They cannot be distinguished on the basis of morphology and are thought to have evolved from *T.b. brucei*, which infects both native and introduced animal species. However, the two species exhibit differences in pathology. *T.b. gambiense* causes a chronic form of the disease commonly known as West African sleeping sickness. *T.b. Rhodesiense*, on the other hand, causes a more acute form of infection, called East African sleeping sickness (5,12,13) (Figure 4). *T.b. Gambiense* invades the nervous system, while *T.b. Rhodesiense* does not ordinarily invade the nervous system but causes death much more rapidly (3,5).

Figure 4

Sleeping Sickness Map

This map shows the geographic distribution of the West African and East African Sleeping Sickness.

African Sleeping Sickness Geographic Distribution Map – WHO - 1999

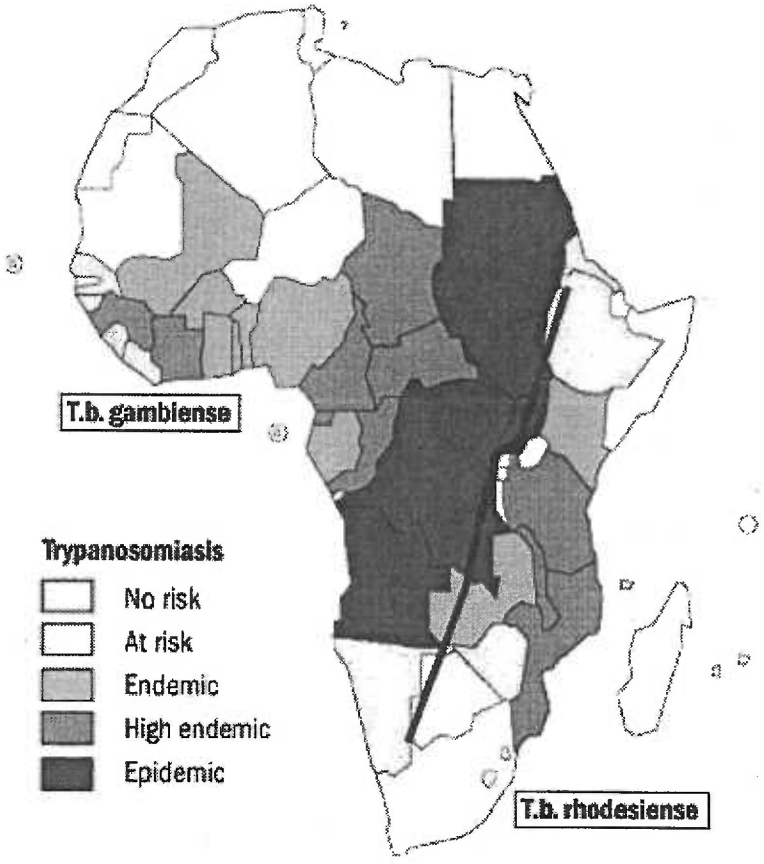

T.b. Rhodesiense causes rapid weight loss and heart involvement and death may occur within a few months of infection; it ordinarily does not cause sleep-walking or other nervous disorders associated with *T.b. Gambiense* because death is usually too rapid for these symptoms to develop (3,5).

T.b. Gambiense invades the central nervous system and this invasion initiates the chronic sleeping sickness phase. Sleepiness and mental dullness increase, accompanied by various nervous disorders, such as tremors, paralysis or convulsions. Coma and death are the final outcomes, unless other opportunistic pathogens or circumstances cause death first (3,5).

a. Life Cycle

Both types of sleeping sickness parasite are transmitted by the bite of different species of the tsetse fly (*Glossina* spp.). The tsetse fly can inject the host with up to several thousand parasites with one bite. Ordinarily a small sore develops at the site of inoculation of the metacyclic trypomastigotes, the infectious form of the parasite. Upon injection, the metacyclic

trypomastigotes transform into the slender trypomastigote form (3,5) (Figure 5). Reproduction is rapid and the parasites invade nearly all organs of the body.

When injested by a susceptible tsetse fly taking a blood meal, *T. brucei* migrates to the midgut, where it multiplies in the trypomastigote form for about 10 days. The trypomastigotes then migrate slowly through the foregut, esophagus, pharynx and finally enter the salivary gland of the tsetse fly. In the salivary gland, they are transformed into the epimastigote form, and after several generations, they change in morphology to the metacyclic trypomastigote (the infectious form). Metacyclic trypomastigotes are small and stumpy and lack a free flagellum (3).

b. Control and Treatment of Sleeping Sickness

Control of sleeping sickness has been attempted by shooting animal reservoirs, using insecticides--first DDT then others, and destruction of tsetse fly habitat (13,14,16).

Figure 5

T. brucei Life Cycle

Life Cycle of African Trypanosomes

Tsetse Fly injects metacyclic trypomastigotes into the host when it takes a blood meal.

Migrates to the salivary glands where it transforms to the epimastigote and then metacyclic trypomastigote form.

The stumpy form is taken up by the Tsetse fly in a blood meal and transforms into the procyclic form and replicates in the midgut.

Metacyclic trypamastigotes transform into slender trypamastigotes then intermediate form and reproduce asexually in the bloodstream of the host

Intermediate form transforms to the stumpy form (vector infective) in the host bloodstream

All of these practices continue to varying degrees. Low-cost tsetse traps impregnated with chemical attractants have been relatively successful in certain regions (15,17).

Early treatment of sleeping sickness is the most effective treatment because after the parasites invade the central nervous system (CNS), the least toxic drugs are no longer effective (6). Arsenical compounds were the first drugs useful against African sleeping sickness. The exact mode of action of the arsenicals remains unclear, but these drugs have been shown to bind non-specifically to disulfide moieties of proteins (18,55). However, a mutated P2 adenosine transporter in trypanasomes has been shown to inhibit the uptake of arsenicals, and may be responsible for drug resistance. This raises significant questions about the mode of action of arsenicals (60).

Melarsaprol B (Mel B) is the arsenical of choice for treatment of sleeping sickness after CNS involvement. Nevertheless, it has some very serious side effects (55). Encephalopathy causes

Figure 6

Drugs used to treat *T. brucei*

Current Drug Treatments for Sleeping Sickness

Taken directly from WHO Fact sheet no. 259 March 2001 – Directly Quoted

"First phase treatments:

Suramine : discovered in 1921, it is used in treatment of the initial phase of *T.b. rhodesiense* . There are certain undesirable effects, especially on the digestive tract.
Pentamidine : discovered in 1941, it is used in treatment of the initial phase of *T.b. gambiense* sleeping sickness. In spite of a few undesirable effects, it is well tolerated by patients. Future production is guaranteed by an agreement between WHO and Aventis.

Second phase treatments

Melarsoprol: discovered in 1949, it is at present the only drug available on the market to treat the advanced stage of sleeping sickness, no matter which parasite is the cause. It is the last arsenical derivative in existence. The undesired effects are drastic; they include reactive encephalopathy (an hyperacute neurological complication of an allergic nature) - often fatal - in 3% to 10% of cases; those who survive the encephalopathy suffer serious neurological sequelae. Furthermore, there is considerable resistance to the drug, rising to 30% in parts of central Africa.

Eflornithine: this molecule, which was registered in 1990, is the alternative to melarsoprol treatment. It is effective only against *T.b. gambiense* . The regimen is strict and hard to apply. Production ceased in 1999. Last year, the company Aventis gave the license to WHO, which has undertaken several initiatives to seek a new source of production.

mortality in between one and five percent of the patients treated. Other side effects include liver and kidney damage. Mel B's advantage over previous arsenicals is that occurrence of ocular nerve atrophy associated with other arsenicals has not been associated with its use (5,18). Eflornithine or DFMO is a newer drug that has been used to treat late stage sleeping sickness. It is active only against *T.b. gambiense*. Eflornithine is an inhibitor of the enzyme ornithine decarboxylase.

Suramin, which is much less toxic to the host than the arsenicals, is the drug of choice for early stage African trypanosomiasis. Suramin is a non-metallic derivative of urea and the mechanism of action is not well understood. In cases where suramin is used early enough its success rate approaches 100%. Side effects include kidney damage, vomiting, and shock (18). The severity of the side effects varies based on the underlying health and nutrition of the patient.

D. *Leishmania*

Six species of the genus, *Leishmania*, are known to cause disease in humans. All of these are obligate intracellular parasites, which are morphologically indistinguishable (3,19). Nevertheless, the disease states caused by different species varies greatly: some species cause a cutaneous form of the disease, which is either treatable or self-limiting; other species, such as *Leishmania donovani*, cause a visceral form of leishmaniasis, which is harder to treat, but with appropriate treatment, a large percentage of patients are now cured (3,19) (Figure 7). All six species are transmitted by the insect vector, commonly known as the sandfly (20). *Leishmania* infects numerous mammalian hosts, which can then act as reservoirs for the parasite. The following discussion will be predominantly limited to *Leishmania donovani*, the causative agent of visceral leishmaniasis.

1. *Leishmania donovani*

In 1903, the causative agent of visceral leishmaniasis was discovered through the combined

Figure 7

Leishmania Species, Geographic Distribution and Diseases

Leishmania Species, Diseases, and Geographic Distribution

Visceral Leishmaniasis

Species	Disease	Geographic Distribution
L. d. donovani	Kala-azar	Middle East, Africa, Asia, Russia, S. America
L. d. infantum	Visceral Infants	Mediterranean
L. d. chagasi	Visceral	South America

Cutaneous Leishmaniasis

Species	Disease	Geographic Distribution
L. tropica minor	Dry Cutaneous	Southern Europe, Middle East
L. tropica major	Wet Cutaneous	Southern Europe, Middle East, Africa
L. braziliensis	Mucocutaneous, Espundia	Mexico, Brazil
L. m. mexicana	Cutaneous, Chicleros ulcer	Central America
L. m. amazonensis	Diffuse, Cutaneous	Amazonas Region

efforts of Dr. Leishman and Dr. Donovan, giving rise to its name *Leishmania donovani* (21). Prior to this time, visceral leishmaniasis was ordinarily misdiagnosed as chronic malaria. *Leishmania donovani* is found in tropical and subtropical parts of the world (21). Current estimates of the number of infections caused by all species of *Leishmania* are 12 million worldwide, and it has been suggested that as many as 350 million people in 88 countries may be at risk (22).

The epidemiology of visceral leishmaniasis is not static and varies greatly over its range. Depending on which region is studied, dogs or rodents play key roles as reservoirs for the parasite. In addition to differences in reservoirs, distinctions in the disease state itself have been noted; for example, in some countries, outbreaks of visceral leishmaniasis are isolated to infants or predominately in children under 10 years old (3,22). The reasons for the observed differences remain unclear; whether there are biochemical variations within the species or biochemical differences in the host or reservoirs

causing these effects has yet to be shown. With the spread of AIDS, co-infection with *Leishmania* has created significant complications, as it appears that the two diseases reciprocally enhance each other. With HIV co-infection, cutaneous forms of leishmaniasis may appear in the viscera, and visceral forms may spread to uncommon locations, including the heart and skin (52).

Visceral leishmaniasis predominantly attacks the liver, spleen, and bone marrow of the host, and if left untreated usually results in death (3,5,21).

a. Life cycle

The bite of the *L. donovani* infected sandfly begins the infection of the human host. The parasite is injected and the parasite is taken up by macrophages attracted to the site of the wound. The parasites are found within the phagocytic vacuoles of the macrophage, where they are transformed from the promastigote, or flagellated form, to the amastigote, or aflagellated form.(3,5) The amastigote multiplies rapidly until the cell is lysed, which allows the amastigotes to spread to

other macrophages. The life cycle continues when a sandfly takes a blood meal from an infected host. Amastigotes are released from the macrophages in the sandfly's gut and are transformed to the promastigote form. The promastigotes migrate to the midgut, reproduce, and mature. The mature promastigotes migrate to the anterior of the sandfly's gut to await the next blood meal in order to infect a new host; this completes the life cycle of the *Leishmania* parasite (3) (Figure 8).

The fact that the parasite infects the macrophage--the immune systems first line of defense--has led to studies of the interaction between the host and parasite. Studies of the pathogenesis of leishmaniasis have led to discoveries regarding the immunological response of the host to the infection (23,24). Perhaps the most interesting question raised by the life cycle is how *Leishmania* can survive within the hostile environment of the macrophage.

Figure 8

Leishmania donovani

Life Cycle

Leishmania Life Cycle

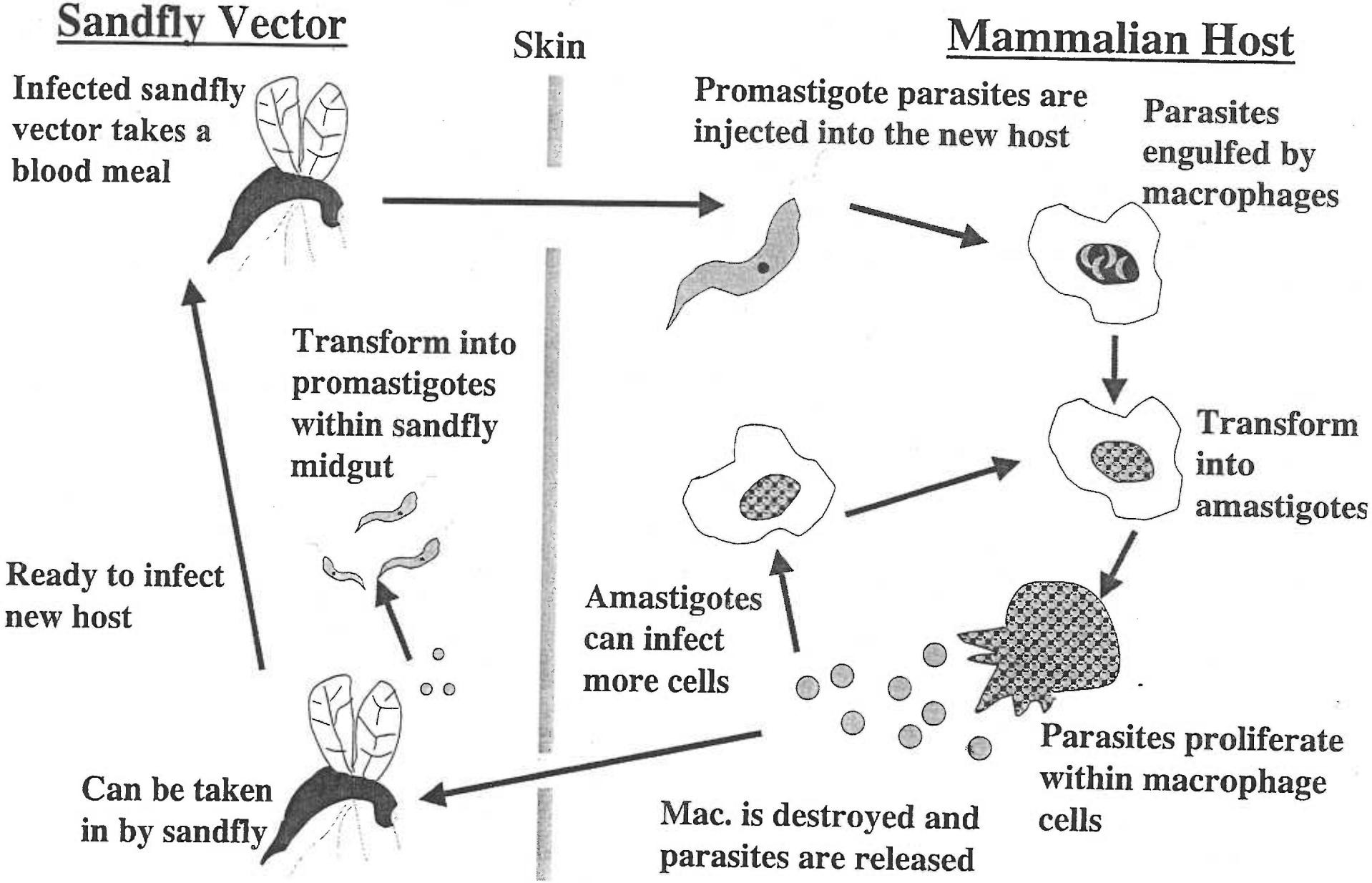

Some studies have suggested that *Leishmania* is able to shut down the macrophages ability to produce lysosomal proteases, while others suggest that Leishmania's cell surface proteins, such as gp63, may protect the parasite (25,26). Research into the survival strategies of the parasite may lead to new vaccines or more effective chemotherapies.

b. Control of *Leishmania donovani*

Attempts to control the spread of visceral leishmaniasis have been of limited success. The best control occurred between 1950 and 1970, when widespread use of DDT to control malaria was attempted; during that time, insecticides had virtually eliminated visceral leishmaniasis in India. However, the adverse effects of DDT have overridden other concerns and incidences of both malaria and leishmaniasis have increased (27).

In addition to insecticides, reduction in incidence of visceral leishmaniasis has been achieved through programs involving reservoir control; in China, one reservoir control strategy consisted of shooting dogs (28). Various other

simplistic approaches have proven to be effective in at least limiting the prevalence of the disease.

c. **Symptoms of and Chemotherapeutic Approaches to *Leishmania donovani***

Visceral leishmaniasis causes a wide variety of symptoms and onset of symptoms is also varied. Visceral leishmaniasis is divided into two stages, the acute and the chronic phase. During the acute phase of the disease, a fever appears and usually spikes twice a day. Diarrhea and vomiting are common along with the enlargement of the spleen and liver leading to death if untreated (3,5).

The chronic form of visceral leishmaniasis is often not diagnosed until it is very advanced. Diarrhea, vomiting and fever are also associated with the chronic phase of the disease, but these symptoms usually become less frequent as the disease progresses. Anemia and gradual wasting often allow opportunistic infections to take hold during the chronic phase of the disease; these opportunistic pathogens are often responsible for the death of the patient, rather than the leishmaniasis itself (6,21).

Treatment of visceral leishmaniasis is based on antimonials, the use of which dates back to 16th century for the induction of vomiting (18). Antimonials are extremely toxic, but are used for leishmaniasis because of their effectiveness. The first antimonial used was the very toxic potassium antimonyl tartrate, followed by less toxic pentavalent antimonials; the most useful are antimonic acid derivatives. However, the precise mode of action of these drugs is unclear. Pentavalent antimonials are less toxic because they are rapidly excreted, but because of their rapid turnover require longer treatment periods (18).

The two prevalently used pentavalent antimonials are sodium stibogluconate (pentostam) and N-methylglutamine antimonite (glucontime). Pentostam is the most widely used drug, although this has nothing to do with the efficacy of the treatments as little difference is perceived. Both compounds are administered intravenously and require hospitalization. The effective dose varies by region, and children often require higher doses per unit of body weight than adults(3,29); this may

would relieve pain by either direct application or ingestion. The early discoveries were made by random testing and observation of the environment. Random testing of compounds for use as treatments of diseases continues to be the most prevalent and successful method for the development of new drugs. In fact, the current WHO strategy for drug development related to tropical diseases uses this as one of the accepted methodologies (34).

Modern drug development is based on the evolution of organic chemistry, which allowed the synthesis of a vast array of new compounds for drug screening. Prior to this, screening of natural compounds was the only avenue to explore. Biochemistry, molecular biology, and pharmacology have also been instrumental in the current drug development revolution; understanding the metabolism of drugs has led to the discovery of numerous useful drugs. Even with all of this new knowledge, discovering new "lead" compounds from which to develop drugs has remained the most time-consuming part of the process. WHO strategies for development of "lead" compounds for tropical

diseases call for *in vitro* testing of compounds to determine efficacy, and then looking for which compounds show no general cytotoxicity to use for further testing (34). This requires screening of potentially very large numbers of compounds just to develop "lead" compounds for further *in vivo* testing.

Early work in the field of drug development by Paul Erlich changed the way scientists viewed the treatment of diseases and the effects of drugs. He emphasized drug selectivity and explored drug/target interactions. Paul Erlich's work on Syphilis was the first step toward a real understanding of the mode of action of drugs and the development of drugs based on selective targeting. Erlich used chemotherapy with arsenic containing compounds to cure syphilis, which is similar to the arsenicals used to treat Sleeping Sickness. He is recognized as the founder of modern chemotherapy (35). This identification of a target and use of a selective medicine for treatment is the precursor to the WHO's second

accepted methodology for developing new anti-parasitic drugs (34).

In 1962, Dr. Woods and coworkers discovered the mechanism of action for sulfonamides. This discovery was the first to show the ability to study the action of drugs on a molecular level (36). Sulfonamides are anti-bacterial and their action on bacteria results from interference with enzyme systems necessary for normal growth, metabolism, and multiplication of bacteria. This groundbreaking work has opened the door to a rational approach to the development of new drugs through understanding the mode of action of existing drugs and the in-depth exploration of disease-causing agents. The WHO's second method specifically calls for identification of molecular drug targets, and then screening large compound libraries to identify compounds that hit the target (34).

The latest approach to drug design is structure-assisted (rational) drug design; this is based on current understandings of biochemistry, pharmacology, and a detailed understanding of the

differences in biochemistry that exist between humans and the disease-causing organisms. This approach has been assisted by developments in molecular biology allowing the cloning and expression of genes; the production and purification of proteins; and through this the elucidation of distinct biochemical pathways within the disease-causing organisms. These distinct biochemical pathways can then be explored to find appropriate target enzymes for the design of drugs that will destroy the disease-causing organism and minimize the impact on the human host.

To pursue x-ray crystallographic structure-assisted drug design, once an appropriate target is discovered, cloning, expression, purification and finally crystallization of the target must be accomplished. However, a myriad of problems may be encountered within each step of this process. Even after crystallization is completed, the crystals must diffract well enough for characterization, and heavy atom derivatives must be prepared in order to phase an initial electron density map. Derivatization and solving the structure are tasks

which can each take multiple years, depending upon the problems encountered (38).

An initial structure generates an image of active site of the target enzyme, and computers can then be used to screen potential inhibitors using docking programs (39). However, in order to design the most effective drugs, the elucidation of the complete enzyme mechanism is required. This may involve crystallographic solutions of the enzyme bound to substrate, substrate analogs, and known inhibitors, and even with all of this information studies of mutants may be required in order to fully understand the enzyme mechanism and design the most effective "lead" compounds.

Once "lead" compounds, active against the target enzyme, are in hand, drug delivery is the next important consideration. Even though a "lead" compound is effective *in vitro*, it may not be able to reach the disease-causing organism within the human host. If it reaches the disease-causing organism, will it get inside of the organism to affect the target enzyme? By the time it travels through the human host and into the disease-causing

organism will it still be effective against the target enzyme? All of these questions must be answered in the affirmative or the drug will have no effect. Most lead compounds will need to be modified substantially to effectively target the organism and enzyme of choice, and efficacy of every modification must be considered; this process is also very lengthy, as many problems may be encountered on the road to solutions.

There are many promising target pathways of interest for attacking parasitic diseases. Two target pathways of interest to the Ullman and Brennan laboratories are the purine salvage pathway (Figure 9) and the polyamine biosynthetic pathway (40,41,42). Clinical trials of allopurinol, a purine analog, which has shown to be metabolized by HGPRT and has efficacy *in vitro* against *Leishmania donovani*, are indicative of the potential promise of the development of better drugs active against the purine salvage pathway or more specifically HGPRT. Recent work in the Ullman and Landfear laboratories on the purine salvage pathway involves elucidation of the mechanism of nucleoside

Figure 9

Purine Salvage Pathway

Purines are taken up by *L. donovani* through its nucleoside transporters. Phosphoribosyltransferases (PRTs) are then used to phosphoribosylate the purines. PRTs are present for hypoxanthine and guanine (HGPRT), xanthine (XPRT), and adenine (APRT). Hypoxanthine is converted to IMP, guanine is converted to GMP, adenine to AMP, and Xanthine to XMP.

Purine Salvage Pathway of L. donovani

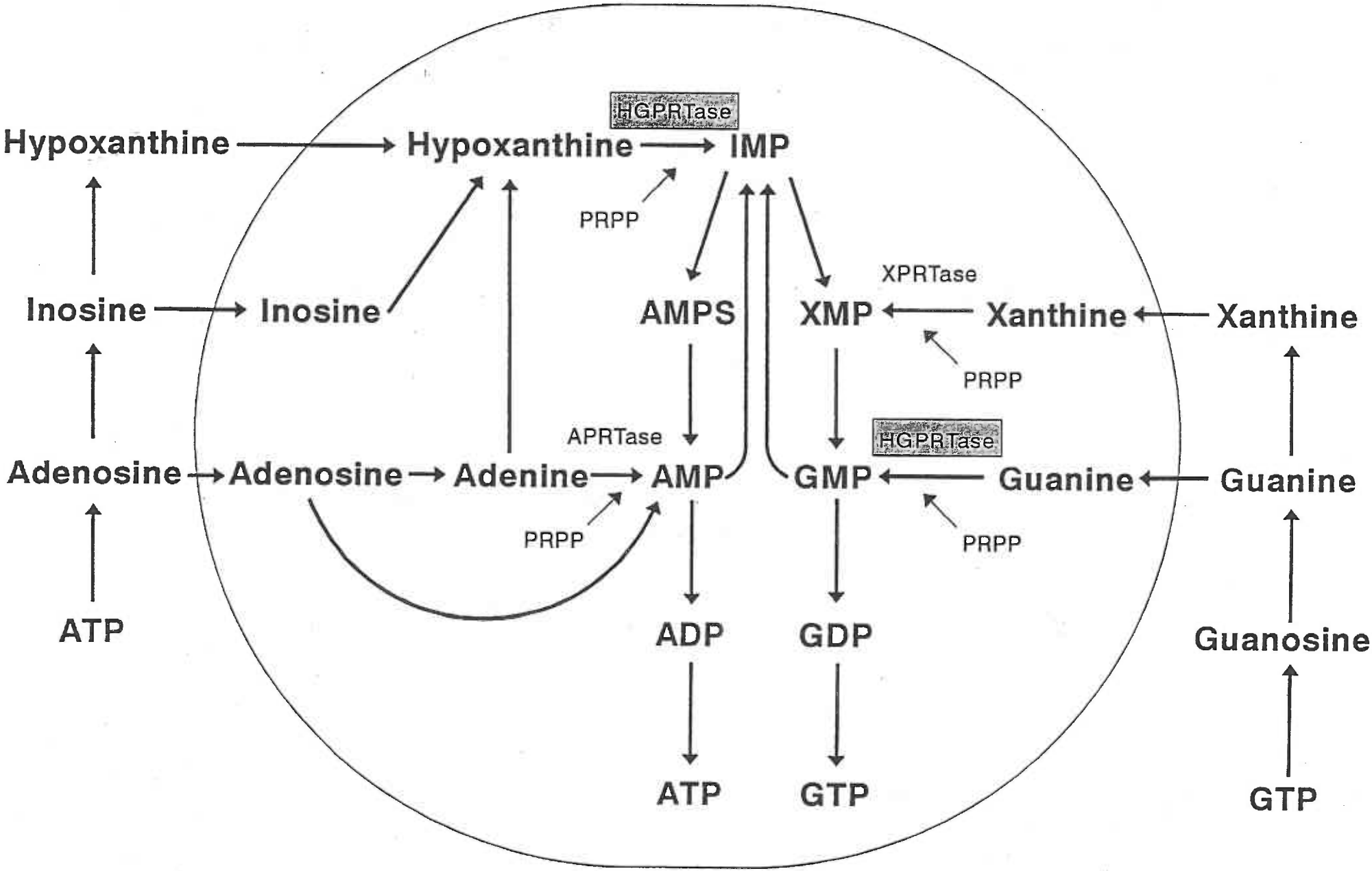

permeation into *L. donovani* by nucleoside transporters (49,61,62).

Difluoromethylornithine (DFMO, also known as Eflornithine) was involved in clinical trials as an antiparasitic drug; DFMO inhibits the enzyme ornithine decarboxylase (ODC), which is a key enzyme in the polyamine pathway and is one of the few new drugs to be introduced in decades. Promising initial results have also been reported for new inhibitors of thymidylate synthetase, an enzyme involved in DNA synthesis, which were developed using a computer-assisted docking program.

The continuing in-depth exploration of the biochemistry of parasites and other disease-causing organisms is certain to expand the list of potential targets for chemotherapeutic intervention; this exploration combined with a better understanding of protein structure and function is sure to eventually lead to the cure of currently incurable diseases for the benefit of future generations.

Purine Phosphoribosyltrasferases from *L. donovani*

Three different purine phosphoribosyltransferases are present in *Leishmania donovani*: 1) Hypoxanthine-guanine phosphoribosyltransferase (HGPRT), which catalyzes the removal of the pyrophosphate moiety from PRPP and the attachment of a purine base, hypoxanthine or guanine, to form a purine nucleotide, IMP or GMP; 2) adenine phosphoribosyltransferase (APRT), which catalyzes the same type of reaction with Adenine and PRPP to form AMP; and 3) Xanthine phosphoribosyltransferase (XPRT), which catalyzes the formation of XMP from Xanthine and PRPP (37) (Figure 10).

Purine phosphoribosyltransferases (*PRT*s) catalyze the addition of the 5-phosphoribosyl group derived from PRPP with purine bases to form 5'-ribonucleotides. These enzymes are the major route through which purines are salvaged. Many parasitic protozoa, including *L. donovani* do not synthesize their own purines and are therefore dependent on the *PRT*s to salvage purines from their hosts.

Figure 10

Reactions catalyzed by the purine phosphoribosyltransferases of *L. Donovani* (45,63).

Reaction catalyzed by HGXPRT

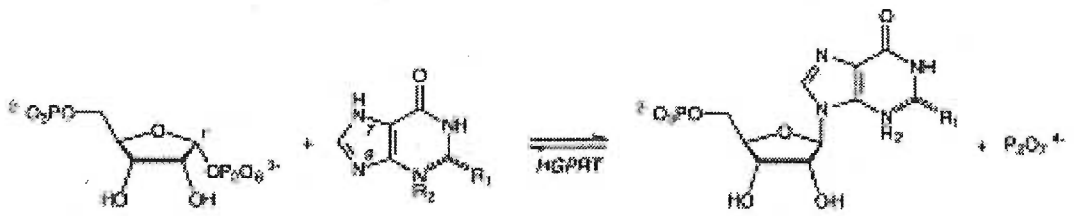

PRPP	Hypoxanthine	R_1 = H	IMP R_1 = H
	Guanine	R_1 = NH_2	GMP R_1 = NH_2
	Xanthine	R_1 =O R_2=H	XMP R_1 =O R_2=H

Reaction catalyzed by APRT

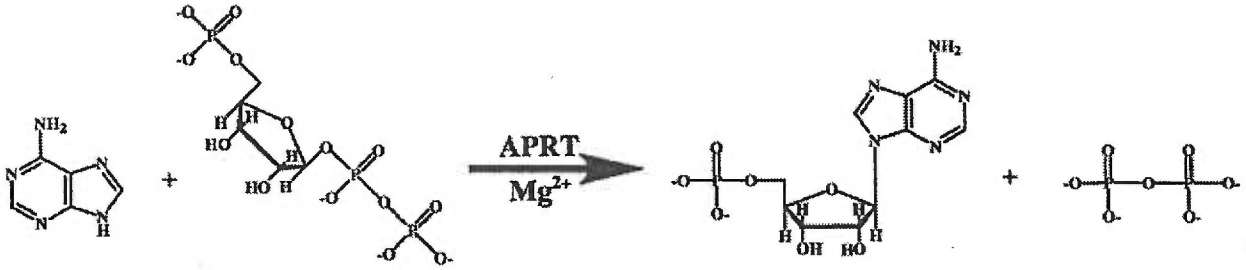

Adenine **PRPP** **Adenosine-5-monophosphate** **Pyrophosphate**

The PRTs are present at high levels in *L. donovani* when compared to mammalian tissues. In fact, the *PRT* levels found in *L. donovani* are close to those found in some bacteria (37). This inability to synthesize purines *de novo* and dependence on *PRT*s for purine salvage makes all of the *PRT*s potentially good targets for drugs designed to inactivate the *PRT* enzymes.

G. Biochemistry of HGPRT

General chemistry teaches that all catalysts work by lowering the activation energy for the reaction they catalyze; an otherwise energetically unfavorable reaction can therefore proceed in the presence of a catalyst. HGPRT is an enzyme that catalyzes the reactions between the purine bases guanine and hypoxanthine and α-D-5-phosphoribosyl-1-pyrophosphate(PRPP) forming purine nucleotides and inorganic pyrophosphate (Figure 11). The discussion that follows will focus on the mechanism through which HGPRT catalyzes the formation of nucleotides, and through what specific amino acid

Figure 11

Reactions catalyzed by HGPRT (45).

Reaction catalyzed by HGPRT

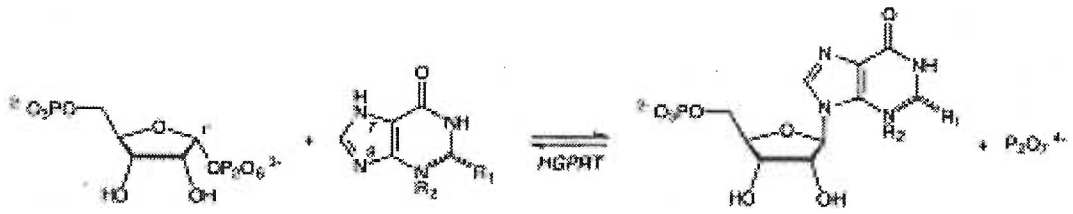

PRPP

Hypoxanthine $R_1 = H$
Guanine $R_1 = NH_2$

IMP $R_1 = H$
GMP $R_1 = NH_2$

contacts and interactions the activation energy of the reaction is effectively lowered to allow the reaction to proceed efficiently. This section is based largely on the work of Heroux, Borhani, *et al.*, who solved the structure of the *T. gondii* HGPRT bound to PRPP and 9-deazaguanine to 1.05 Å resolution (45).

The HGPRT enzyme consists of a large lower "core" domain and a smaller upper "hood" domain; the substrates occupy the active site which is located between the "hood" and "core" domains (45). A large flexible loop (loop II) becomes ordered and locked over the substrates only upon the binding of both substrates in the active site; this flexible loop consists of a 2 strand parallel β sheet with a 90 degree bend in its center (45) (Figure 12).

Geometrical distortions in PRPP substrate

One of the primary ways that HGPRT lowers the activation energy of the reaction appears to be

Figure 12

T. gondii HGPRT Secondary and Tertiary Structures.

Figure(a)shows the GMP complex with loop II open (45).

Figure (b) shows the Mg^{2+}-PRPP/9-deazaguanine ternary complex. Substrates are depicted as space filling models in the active site, between the "hood" and "core" domains. Helices are lavender, β strands are green, and the five active site loops are shown in red. Loops II and III' close over the active site upon formation of the ternary complex (45).

Hood/Core structure – open and closed flexible loop II

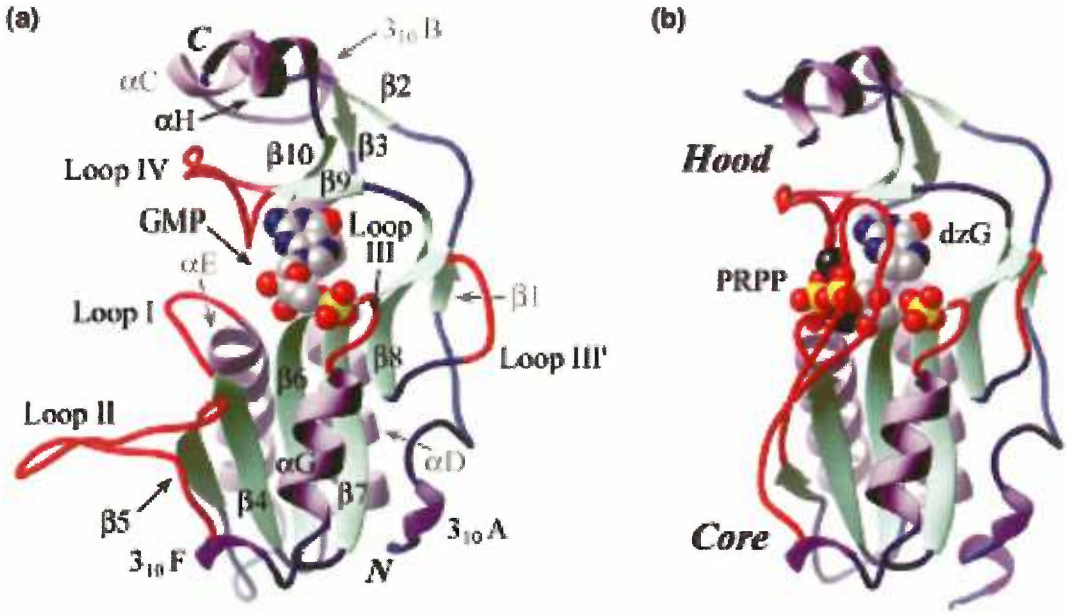

through forcing the PRPP substrate into a higher energy geometry, which assists in the reaction required bond cleavage and ionization of the pyrophosphate and ribose phosphate (45).

In its enzyme bound form, the pyrophosphate group's geometry is altered in three significant ways: 1) the pyrophosphate bridging oxygen atoms bonds to the phosphates on both sides are not equal in length; 2) the bond angle at the bridging oxygen atom is smaller than expected at 127.6° versus the expected >130°; and 3) the bond angles around the ribose-proximal phosphorus atom are far from tetrahedral with compression between the ribose attached oxygen and pyrophosphate bridging oxygen bringing that bond angle to approximately 99.0°, and widening the angle between the non-bridging oxygen atoms to 117.7°. The terminal PO_3 is very close to tetrahedral (45) (Figure 13).

Two coordinated Mg^{2+} ions each have 6 oxygen ligands. However, their geometries vary significantly. Mg1 has O-Mg-O bond angles from 156° to 171.3° in contrast to the expected

Figure 13

The Active Site of *T. gondii* HGPRT

The active site including electron density of both substrates, Mg^{2+} ions, and water molecules, and showing hydrogen bonding within the active site (45). Note the location and hydrogen bonding of K178—this is the equivalent lysine to K-157 in *L. donovani* HGPRT.

Active site of HGPRT

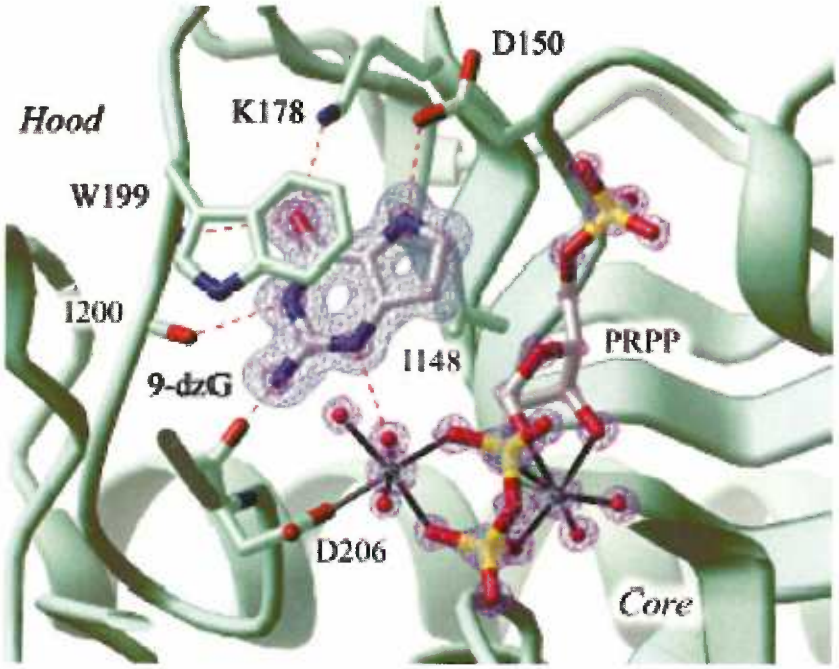

180°, and bond distances of 1.97-2.29 Å (45). The bond angle distortion appears to be caused by its simultaneous coordination to three oxygens in the PRPP molecule (Figure 14). This distortion extends to a conserved Glu residue (Glu 146) through a water molecule bonding the Glu residue to the Mg1 ion. This Glu residue exists in two equally populated alternate forms, one with a favorable side chain torsion angle, and one with a high energy side chain torsion angle. The second Mg ion, Mg2 is much closer to the expected geometry with Mg-O distances ranging from 2.04-2.14 Å and bond angles between 171.9° and 178.9° (45).

The geometrical distortions shown in the enzyme-bound form of PRPP raise its energy, and allow it to overcome what would ordinarily be the more favorable direct and water mediated interactions between Mg^{2+}-PRPP and HGPRT; this is particularly notable in the distortion of the highly charged pyrophosphate group, as charge/charge and hydrogen bonding interactions

Figure 14

Open stereoview of substrates in the *T. gondii* HGPRT active site.

9-Deazaguanine, PRPP, Mg^{2+} ions and associated water molecules are shown in the orientation found in the ternary complex (45).

Open View of Substrate alignment

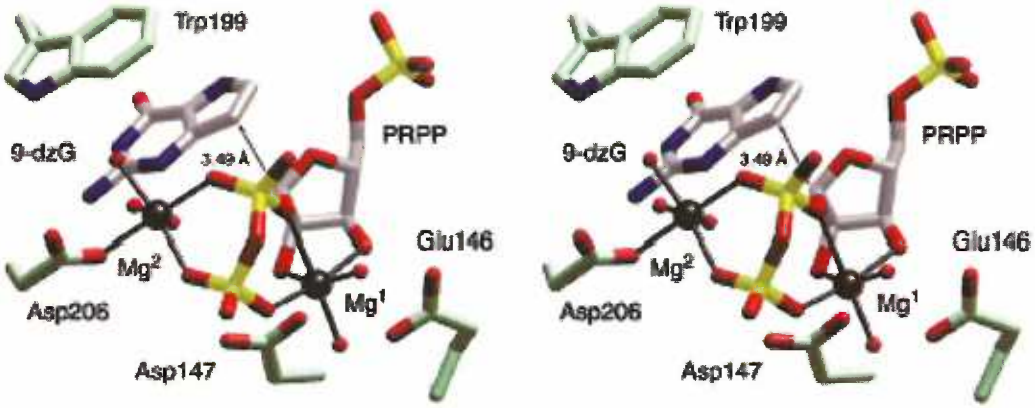

would be stronger relative to the pyrophosphate moiety (45).

One additional energetic consideration involves the pyrophosphate group as well. In its enzyme-bound form, the non-bridging oxygen atoms are forced into a high energy almost eclipsed conformation with approximately a 10° stagger (45) (See Figure 14).

Based on the high energy geometric distortions to the PRPP substrate, it appears that the free energy of substrate binding is used to distort the molecular geometry of the PRPP substrate to approach transition state geometry and favor the catalyzed reaction (45).

Another geometric distortion involves a distinct and unusual ribose ring pucker, which are evident in the enzyme-bound form of PRPP(45). The C2' atom lies 0.54 Å above the plane formed by the four other ribose ring atoms (Figure 15). It has been suggested that this C2' endo conformation is energetically destabilizing and raises the energy of the bound substrate toward transition state energy (45). It appears that this pucker may be

Figure 15

Ribose Ring Puckering.

This figure shows the ribose ring in the *T. gondii* HGPRT with its unexpected C2'-*endo* conformation (45). The C2' atom lies 0.54 Å above the plane formed by the other four members of the ribose ring (45).

Ribose Ring Puckering

(a)

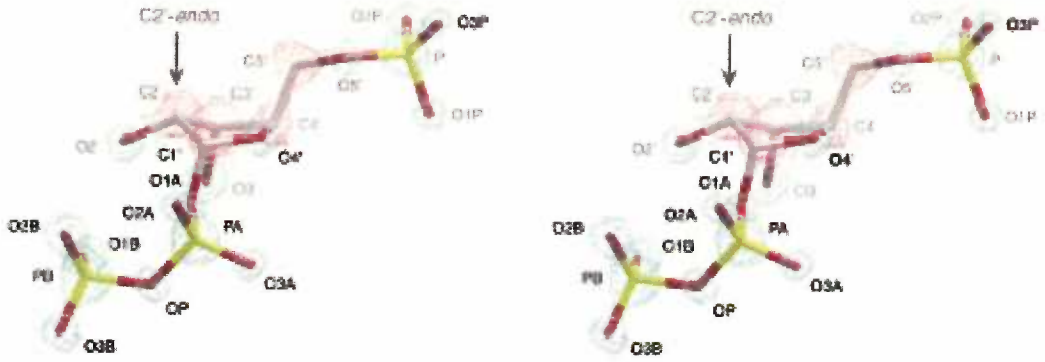

related to the compression of the bond angle at the ribose-proximal phosphate and due to the O3' and O1A bonding to the Mg1 ion creating the distortion in both the PRPP and the Mg1 bond angles, thereby causing the torsion which may explain the puckering effect observed (See Figure 15). The strain created on these PRPP substrate bonds may act to close the gap between the ribose phosphate and the purine base upon ionization of the pyrophosphate group by creating a spring-like effect upon release of the pyrophosphate group pushing the ribose ring in an upward direction and appropriate orientation while still partially bonded to the enzyme; it may push it directly toward the still fully enzyme-bound purine to assist in completion of the reaction. Heroux, Borhani, *et al.* (45) suggest that the ribose phosphate moves up to complete the bond with the purine, because the purine is tightly bound by the enzyme, and the pyrophosphate is also tightly bound. It would be interesting to attempt to take a crystallographic look at an HGPRT bound ribose-5-phosphate and 9-deazaguanine to see a snapshot of the conformation the ribose-5-phosphate

would end up in after ionization of the pyrophosphate group; however, this may not be possible because it may cause the release of the substrates and opening up of flexible loop II.

Electronic interactions

The ground state of PRPP is further destabilized in its HGPRT-bound form by the short distance (2.88Å) between O4′ and O5′ oxygen atoms (Figure 16). These oxygen atoms repel each other and O4′ is pushed away from O5′ and toward C1′ closer to the transition state; O4′ electrons help to stabilize the formation of the positive charge created by formation of the *oxocarbenium* ion at C1′ upon ionization of the pyrophosphate group (45). However, it appears that the primary stabilization of the transition state formation of the *oxocarbenium* ion is achieved through π-cation interaction with a conserved tyrosine residue with its aromatic ring oriented toward the C1′ and O4′ atoms on the PRPP; the delocalized π electrons of the aromatic ring help to electrostatically stabilize the formation of the positively charged

Figure 16

Electronic Interactions in the *T. gondii* HGPRT Active Site.

Figure 16(a) depicts destabilizing nonbonded electron interactions between the O4′ and O5′ atoms, which make a close approach in the active site evident in Figure 16(b) (45).

Figure 16(b) shows "stabilizing cation-π interaction between PRPP and Tyr-118. PRPP, 9-dzG, Tyr-118, and Trp-199 are shown as ball-and-stick models. Note the close approach of the aromatic ring of Tyr-118 to the C1′ and O4′ atoms of PRPP, the site of oxocarbenium ion formation in the transition state. The cation-π donating ability of Tyr-118 is increased by a possible low-barrier hydrogen bond to the PRPP 5′-phosphate group. This hydrogen is shared nearly equally between Tyr-118 (oxygen atom OH) and PRPP (oxygen atom O3P)" (45).

Oxocarbenium Ion Formation

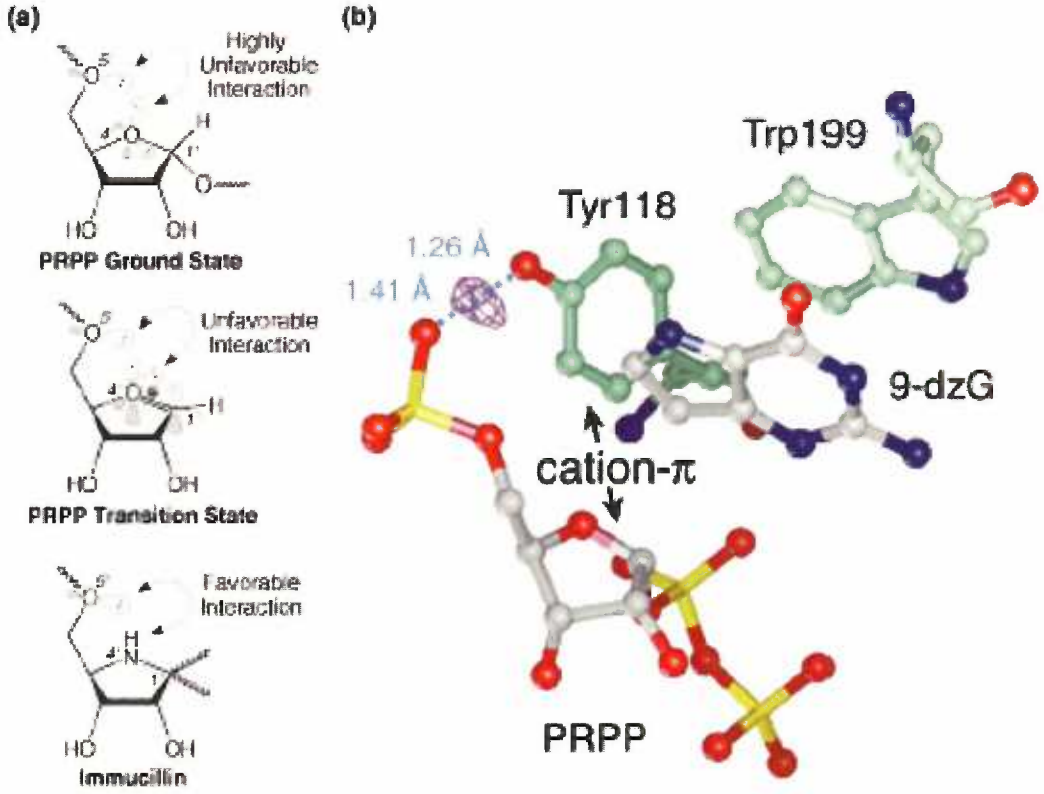

oxocarbenium ion in the transition state (58). This tyrosine residue is further coordinated with a tryptophan residue that lies directly over the purine base in the *T. gondii* HGPRT (45). This coordination of two aromatic residues enhances the stabilizing effect (57). Furthermore, the tyrosine residue forms a short hydrogen bond to the 5' phosphate of the PRPP, where the hydrogen atom is almost equally shared between the two oxygen atoms (See Figure 16); this appears to withdraw the hydrogen atom's positive charge characteristics away from the tyrosine residue giving an overall greater negative charge character to the aromatic ring and allowing greater stabilization of the *oxocarbenium* cation in the transition state, while also assisting in stabilization of the negatively charged pyrophosphate (45). It should be noted that site directed mutagenesis of this conserved tyrosine residue in *L. donovani* HGPRT drastically lowered enzymatic activity, further supporting the suggested role of tyrosine stabilizing the transition state oxocarbenium cation formation (40).

It appears that most of the other conserved amino acid residues involved in hydrogen bonding to the substrates, such as the conserved lysine residue, assist in catalysis by binding both substrates in the optimal orientation for the reaction to proceed (See Figure 13). A conserved Asp residue is involved in hydrogen bonding to the the purine N7, assisting in the bonding of the C1' of the ribose phosphate to the purine N9, while the Mg^{2+} ions help stabilize pyrophosphate ionization (45). In *T. gondii* HGPRT, the polarity of the active site is further enhanced by five aspartic and glutamic acid residues (-5 charge), four lysine and arginine residues (+4 charge), and the pyrophosphate (-3 charge) along with ten water molecules; this enhanced polarity of the active site assists in the ionization of pyrophosphate, in a similar fashion to the interactions between polar solvents and polar solutes (45).

The closure of loop II appears to be critical for catalysis. The interaction of the critical conserved tyrosine residue comes from this loop II closure (45). Loop II also joins the core

and the hood domains and appears to compress the active site placing the C1' of the PRPP closer to the purine N9 reaction site (45) (See Figures 12 and 14). Loop II forms extensive interactions with the hood domain through 6 hydrogen bonds, a double salt brige, and van der Waals contacts (45). It appears that the free energy released through these extensive loop II interactions with the hood domain compress the substrates and assist greatly in effectively lowering the activation energy of the reaction by forcing the substrates close to transition state geometry, and closing the gap between the purine base and PRPP.

Function of conserved Lysine residue in HGPRTs

Around the time of the site-directed mutagenesis work performed in this thesis, Eads *et al.* (43)solved the crystal structure of human HGPRT with bound GMP to 2.5 Å resolution. The GMP molecule binds in an anti conformation in a solvent-exposed cleft of the enzyme. The authors suggested that the Lys-165, which forms a hydrogen bond to O6 of GMP, was critical for determining the specificity of the enzyme for guanine and

hypoxanthine over adenine.(43) Adenine has an NH_2 group in the 6 position. In order to test this hypothesis, the equivalent *L. donovani* HGPRT residue Lys-157 was chosen for site-directed mutagenesis.

Subsequent structural work by Focia *et al.* (44). in 1998 solved the crystal structure of *T. cruzi* HGPRT bound to the inosine analogue, formycin to 1.4 Å resolution, which showed the same type of bonding with its equivalent Lys-143 H-bonded to the carbonyl oxygen at purine position 6.(44) *T. gondii* HGPRT was also solved in the year 2000 by Heroux, Borhani *et al.* (45) to 1.05 Å bound to Mg^{2+}-PRPP and 9-deazaguanine (9-dzG). The *T. gondii* structure also confirmed the role of the conserved lysine; in *T. gondii*, Lys-178 formed a hydrogen bond with the O6 residue of the deazaguanine (45).

Structural work on *PRT*s also confirmed that *PRT*s exist as dimers and tetramers. All of this structural work suggests that the main role of most of the amino acids bound to the substrates are optimal orientation of the substrates for reactivity; this appears to be the primary role of

the Lys-157 in *L. donovani* in addition to its role in substrate recognition (48).

H. Materials and Methods

HGPRT Purification

Recombinant *L. donovani* HGPRT was purified using the method described by Allen *et al.* (46). 500 mL cultures of transformed SΦ606 *E. coli* were grown for 12 hours at 37 °C to an OD_{600} = 0.9-1.2. The cells were centrifuged and then washed several times with phosphate buffered saline (137 mM NaCl, 2.7 mM KCl, 8.1 mM Na_2HPO_4, and 1.0 mM KH_2PO_4). The cells were then suspended in a 20 mM Tris at pH 7.4, 5 mM $MgCl_2$, and 1 mM dithiothreitol (TMD Buffer). The cells were lysed using a French press and then centrifuged at 30,000 x g for 30 minutes at 4 °C. The supernatant was collected and chromatographed over a 10 mL GTP agarose affinity column. The column was washed with a minimum of 100 mL of TMD buffer and the recombinant HGPRT was then eluted in TMD buffer containing 1 mM PRPP. The eluted enzyme was then dialyzed in TMD buffer to remove the PRPP.

Crystallization

The *L. donovani* HGPRT was crystallized by hanging drop vapor diffusion method in a solution of 0.1 M Hepes buffer at pH 7.5 and 0.75 M $LiCl_2$; the size of the initial crystals were approximately 0.2 mm by 0.1 mm and the shape was hexagonal bipyramidal. After more experimental work, the size of the crystals was doubled to 0.4 mm by 0.2 mm. *T. cruzi* and *T. brucei* HGPRT crystallizations were attempted under a variety of conditions using the hanging drop vapor diffusion method but never yielded anything but small needles or small rod-shaped crystal, which were unsuitable for further study.

Site Directed Mutagenesis

L. donovani HGPRT mutants were generated by subcloning the *EcoR-XbaI* cleaved fragment from the HGPRT-pBAce construct described by Allen *et al.* into the corresponding sites in the pSelect mutagenesis vector (Promega) (46). The vector DNA was transformed into competent cells of JM109, and recombinant colonies were selected by plating on LB plates containing 12.5 µg/mL tetracycline. The

EcoRI-XbaI fragment contains the entire HGPRT coding region, as well as the *phoA* promoter, allowing expression of the mutated genes and protein production in *E. coli* without further subcloning.

Site-directed mutagenesis to create single amino acid substitutions were introduced into the HGPRT gene with 25-base pair mutagenic oligonucleotides containing the appropriate base replacements centrally located in the primer following the protocols outlined in the brochure provided by Promega, which includes repair of an ampicillin resistance gene allowing for selection on LB ampicillin plates. The mutated genes were then sequenced for verification.

Complementation Studies

Complementation analysis was performed with both wild type and mutant HGPRT-pSelect constructs by transformation into SΦ609 (Δ*pro-gpt-lac, hpt, thi, pup, purHJ*) *E. coli*; SΦ609 *E. Coli* is a purine auxotroph that lacks HGXPRT activity. Transformants were isolated on LB plates containing 100 µg/mL ampicillin and 50 µg/mL streptomycin.

Initial complementation analysis was performed on LB plates containing 100 μM ade/gua, ade/hyp, or ade/xan to test for complementation with guanine, hypoxanthine, and xanthine. Adenine complementation was tested for in a cell line that is deficient in APRT activity *E. coli* SΦ446, and adenine was added to the LB plates and wild type and all mutant enzymes were tested. Single bacterial colonies transformed *E coli*. SΦ609 from the wild type and each mutant were picked and resuspended in 200 μL of low phosphate induction (LPI) medium supplemented with 100 μg/mL ampicillin and 50 μg/mL streptomycin (10). Twenty μL aliquots were then dispensed into 3.0 mL of LPI medium containing both antibiotics and adenine, with hypoxanthine or guanine. Each nucleobase or nucleoside was present at a concentration of 100 μM. Cultures were incubated at 37 °C with vigorous shaking for 48 h. and abs 600 measurements were taken of the cultures at multiple intervals for comparison purposes.

Kinetic Measurements

Steady state kinetics of HGPRT comprising rate measurements for the forward reaction were determined using a 1.0 cm path length on a Beckman DU640 spectrophotometer equipped with a kinetic software package allowing determination of Michaelis-Menten kinetic values. Km and Vmax values for the wild type and mutant HGPRT proteins were determined. Reactions were carried out in 100 mM Tris-Hcl, pH 8.0, 10 mM $MgCl_2$, 2.0 mM dithiothreitol at 37 °C either in 1.0 mM PRPP and 1 to 100 μM guanine or hypoxanthine to determine the Km for the base. IMP and GMP formation were monitored at 243 and 257 nm, respectively, using extinction coefficients of 2200 M^{-1} cm^{-1} and 4200 M^{-1} cm^{-1}, respectively.

I. Results

Recombinant wild type *L. donovani*, *T. cruzi*, and *T. brucei* HGPRTs were produced in the pBace expression vector (under control of the phoA promoter) in SΦ606 *E. coli* cells. One step purifications were performed using GTP-agarose affinity chromatography. These purified proteins

were then used for crystallization experiments (Figure 17 and 18).

Crystallization experiments were carried out for the *L. donovani*, *T. cruzi*, and *T. brucei* HGPRTs as a starting point for overall structure determination. *T. cruzi* and *T. brucei* HGPRTs yielded only small rod-shaped crystals, which were unsuitable for crystallographic analysis (Figure 17). The *L. donovani* HGPRT was crystallized by the hanging drop vapor diffusion method in a solution of 0.1 M Hepes buffer at pH 7.5 and 0.75 M $LiCl_2$; the size of the initial crystals were approximately 0.2 mm by 0.1 mm and the shape was hexagonal bipyramidal (Figure 18). The initial crystals diffracted to approximately 7-8 Å. After more experimental work the size of the crystals was doubled to 0.4 mm by 0.2 mm, but the crystals still diffracted to a maximum of 5-6 Å. Preparative isoelectric focusing of the protein was completed to further purify the protein to one isoelectric species in an attempt to improve the

Figure 17

T. cruzi HGPRT crystals

Crystals

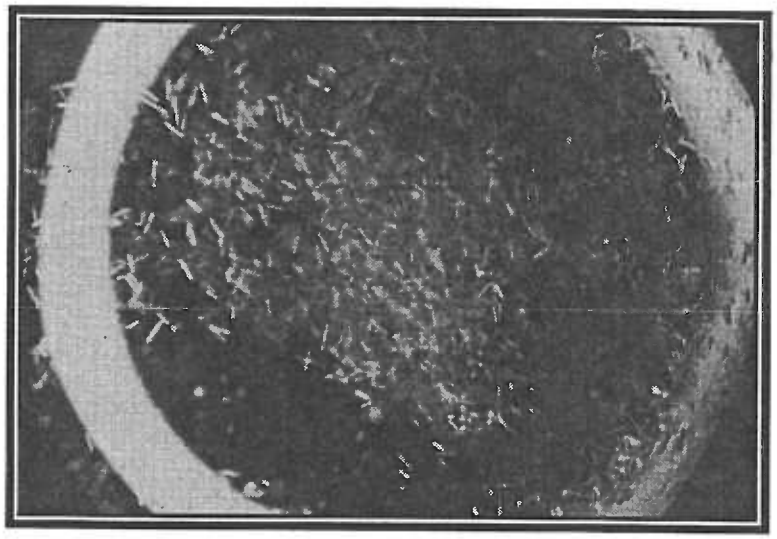

Figure 18

L. donovani HGPRT Crystals

Crystals

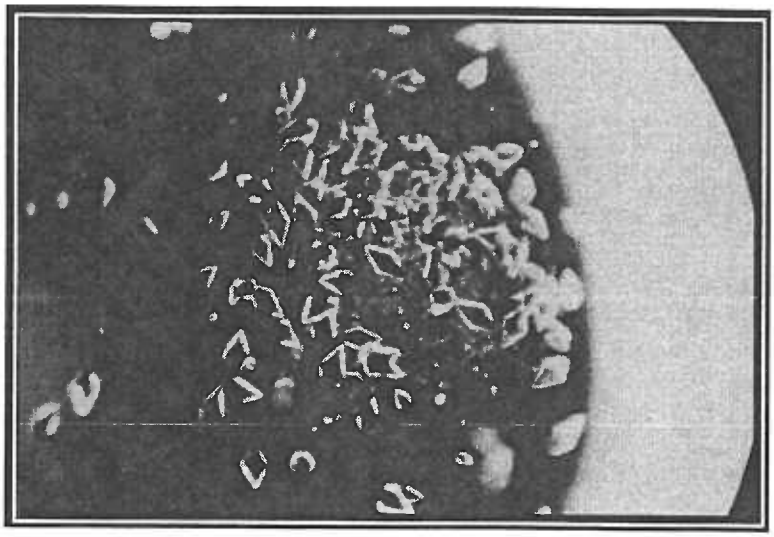

diffraction quality of the crystals (Figure 19); the strongest band on the 6-8 gel was used for crystallization, but this attempt failed at improving the packing of the crystal and diffraction resolution did not improve. Therefore, molecular modeling of all three enzymes, based on the solved structure of the human HGPRT was completed, and site-directed mutagenesis studies of an active site residue of the *L. donovani* enzyme were started (Figure 20).

Eads et al. had solved the human HGPRT structure and suggested a mechanism through which the equivalent lysine in the human enzyme to the Lys-157 in the *L. donovani* HGPRT played a key role in the specificity of the enzyme for guanine and hypoxanthine over adenine based on the role of lysine in hydrogen bonding the O6 of guanine and hypoxanthine in comparison to the amino group at that position in adenine. No mutagenic studies were completed on the human enzyme. In order to explore the role of lysine 157, five separate mutations of lysine 157 were created; lysine 157

Figure 19

Isoelectric Focusing of wild type *L. donovani* HGPRT.

Isoelectric Focusing of HGPRTase

6-8 IEF Gel

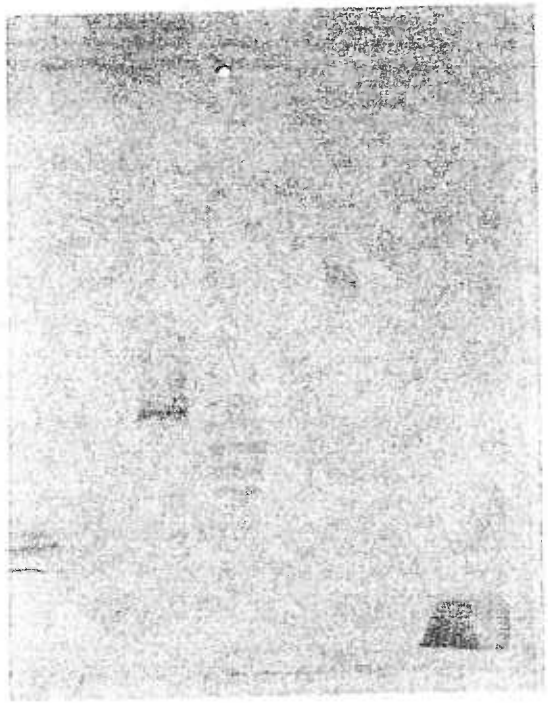

3-10 IEF Gel

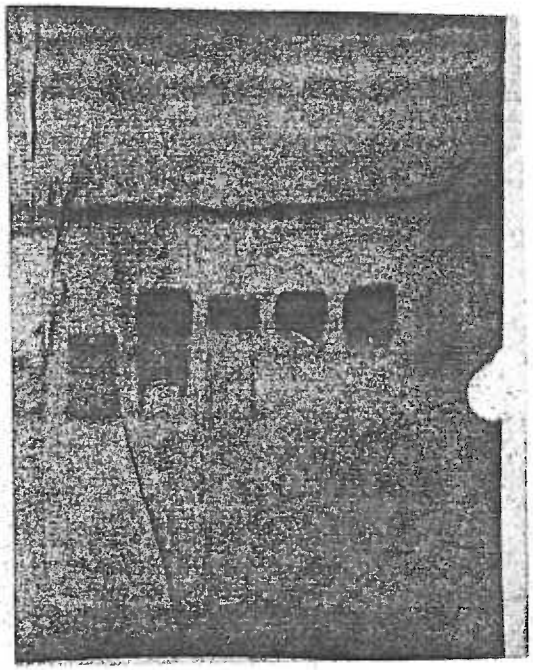

Figure 20

Molecular Model of *L. donovani* HGPRT active site compared to crystal structure of the human enzyme, upon which the model was based.

Comparison of *L. donovani* HGPRT active site model and solved human crystal structure active site

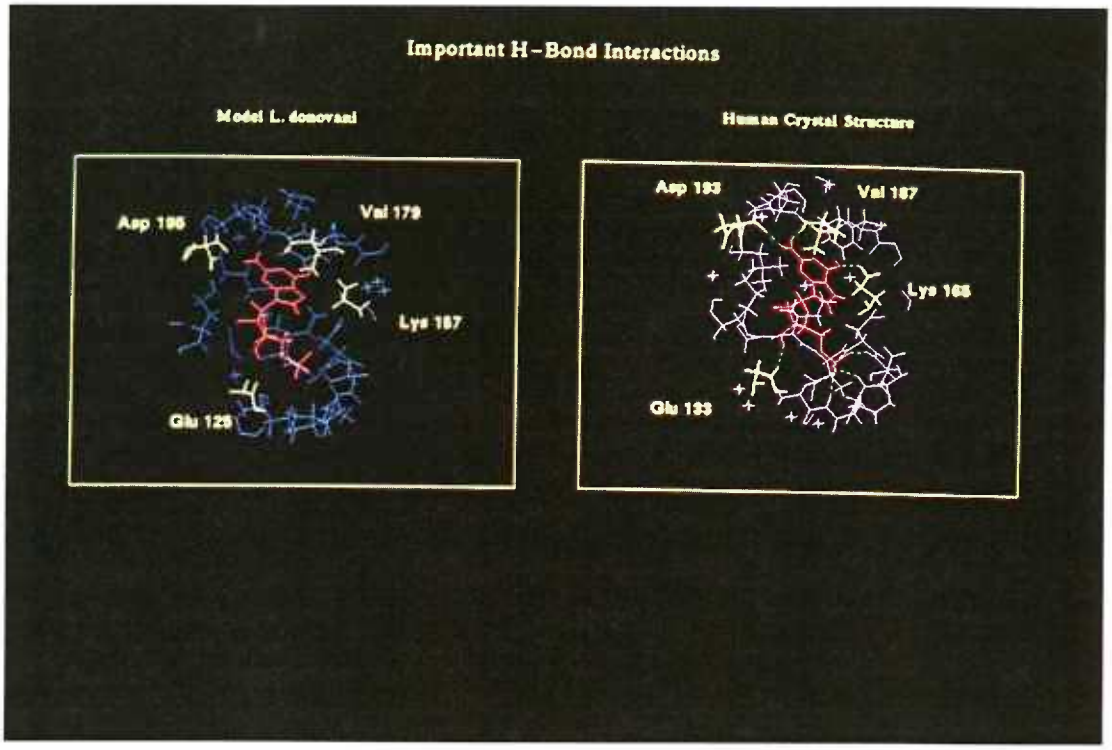

was mutated to alanine, arginine, glutamine, glutamic acid, and methionine.

Complementation studies were performed using a transformed auxotrophic bacterial strain lacking HGXPRT activity: *E. coli* SΦ609 cells, showing that all of the mutations of lysine 157 did not allow complementation in guanine or xanthine, but the alanine and arginine mutations still allowed weak complementation in 100 μM hypoxanthine when plated out or grown in liquid media (Figure 21).

Adenine complementation was tested on wild type and all 5 mutants transformed into *E. Coli* SΦ446, an *aprt* deficient cell line. Neither the wild type enzyme nor any of the mutants showed any growth with adenine. The wild type and all mutant enzymes were produced in the *E. coli* SΦ609 cell line and all were purified in one step on a GTP-agarose affinity column (Figure 22).

Kinetic studies were then undertaken to determine the K_m for hypoxanthine and guanine for the wild type enzyme and all of the mutants. The

Figure 21

Complementation Studies

The following graphs show growth of transformed SΦ609 *E. coli.*: (A) The first graph shows the positive control with adenine and guanosine added to the growth media, and the negative controls with no purine added to the growth media; (B) The second graph show guanine added to the growth media; Lines with no growth are eclipsed—any lines that are not visible are at zero; and (C) The third graph shows hypoxanthine added to the growth media; again, lines with no growth are eclipsed and are at zero.

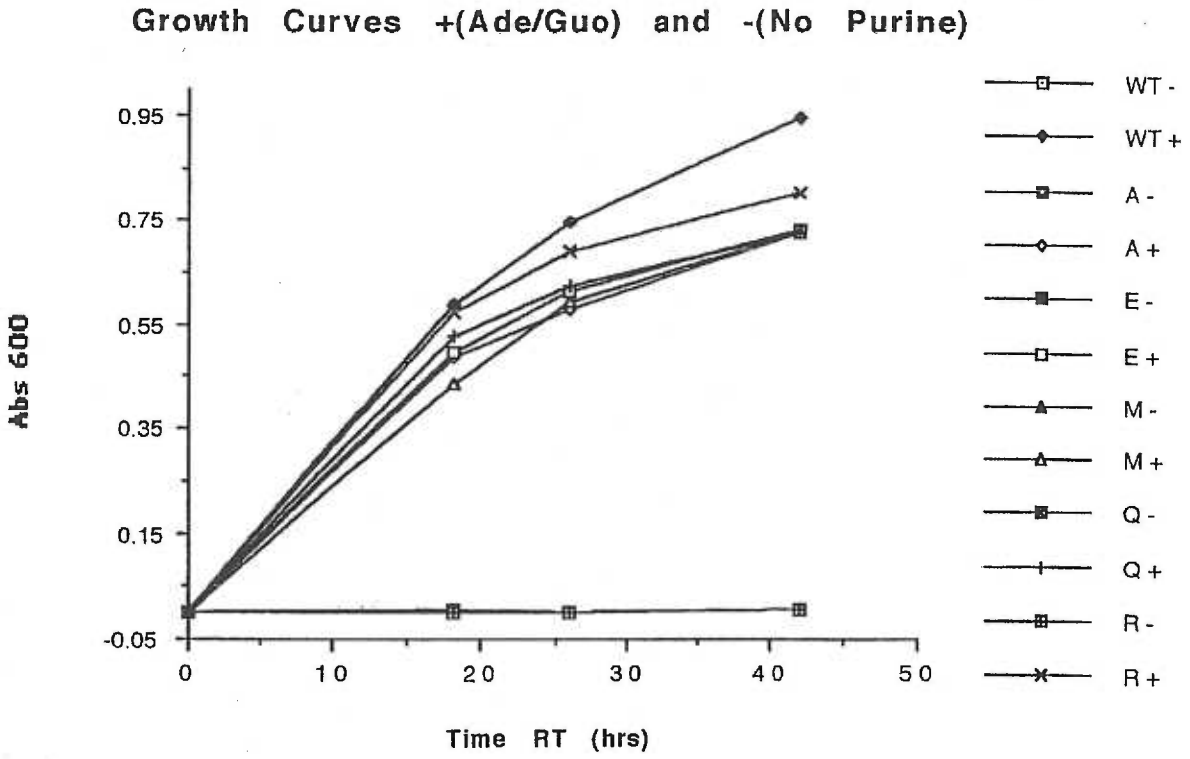
Growth Curves +(Ade/Guo) and -(No Purine)
Abs 600
0.95
0.75
0.55
0.35
0.15
-0.05
0
10
20
30
40
50
Time RT (hrs)
WT -
WT +
A -
A +
E -
E +
M -
M +
Q -
Q +
R -
R +

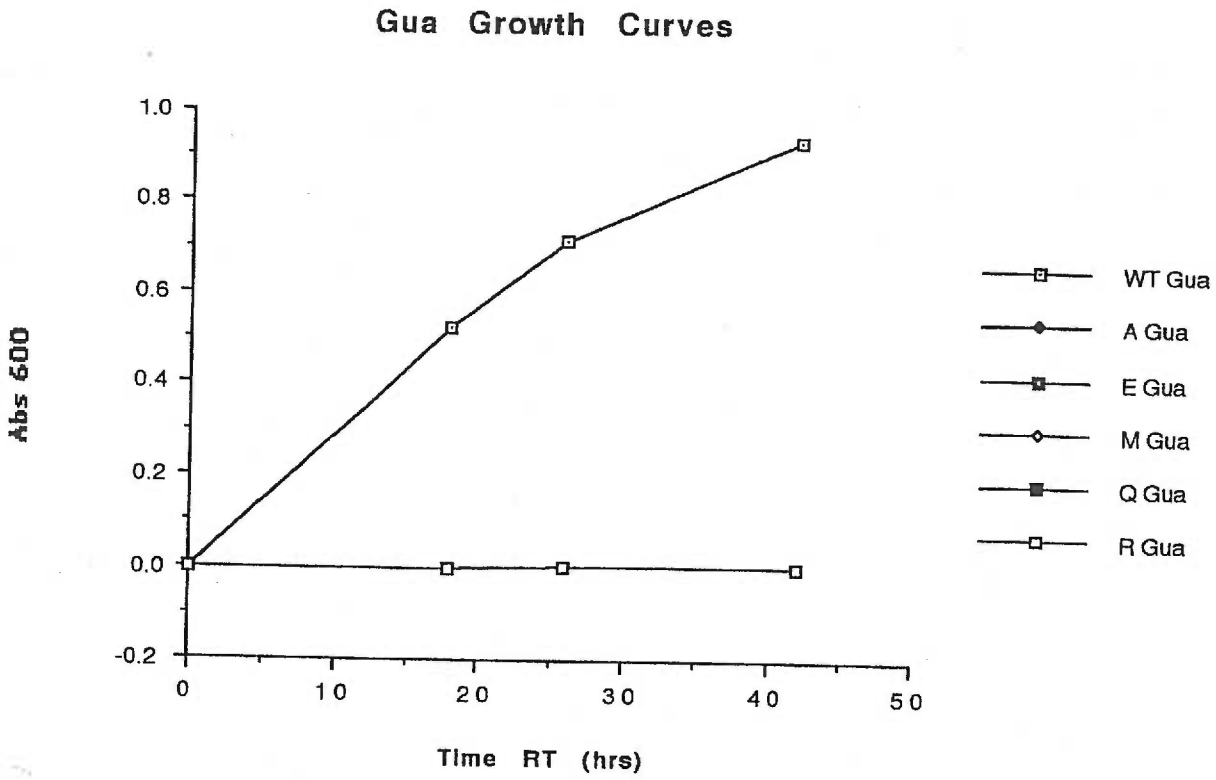
Gua Growth Curves
Abs 600
1.0
0.8
0.6
0.4
0.2
0.0
-0.2
0
10
20
30
40
50
Time RT (hrs)
WT Gua
A Gua
E Gua
M Gua
Q Gua
R Gua

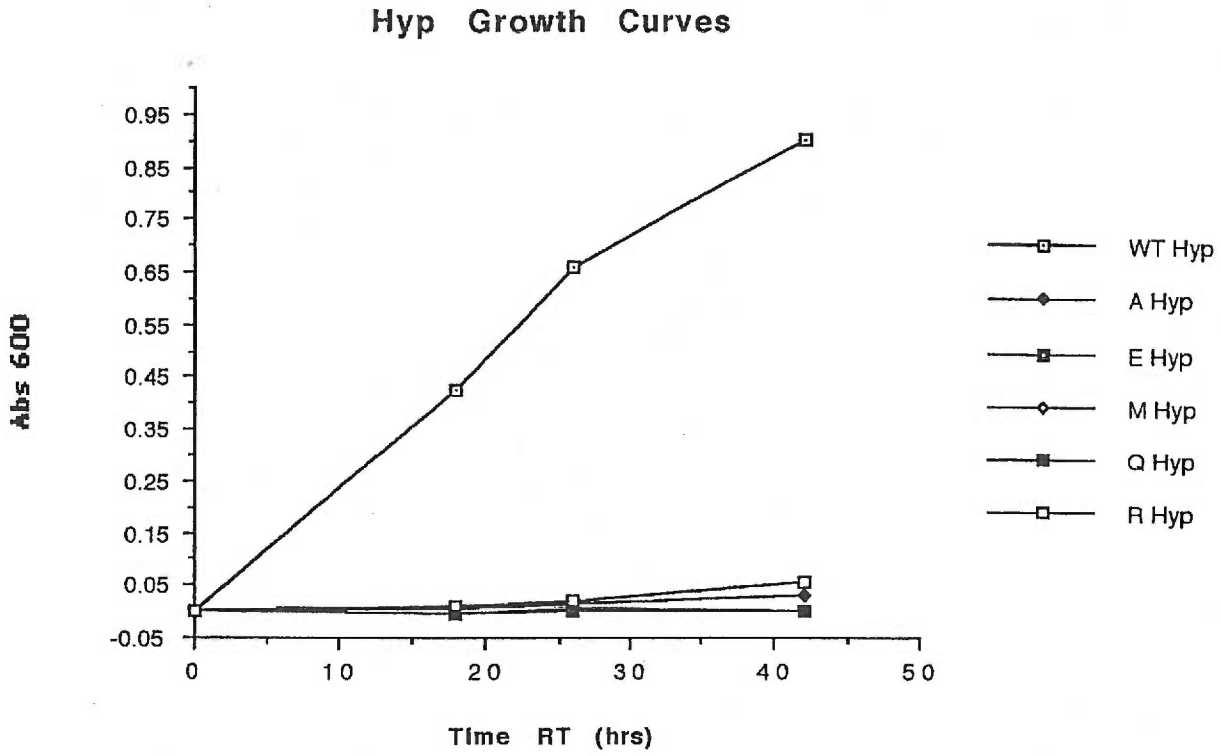
Hyp Growth Curves
Abs 600
0.95
0.85
0.75
0.65
0.55
0.45
0.35
0.25
0.15
0.05
-0.05
0
10
20
30
40
50
Time RT (hrs)
WT Hyp
A Hyp
E Hyp
M Hyp
Q Hyp
R Hyp

Figure 22

Purification of wild type and mutated HGPRT proteins

All proteins were purified in one step on a 10 mL GTP-agarose affinity column, washed with at least 100 mL of TMD Buffer and then eluted with PRPP. After elution, all proteins were dialyzed in TMD buffer to remove the PRPP used in the elution. The top SDS-PAGE gel shows the crude lysate cell extract following protein production. The bottom gel shows the purified proteins following GTP-agarose chromatography. The standards shown are in kDa measurements.

L. donovani HGPRT crude lysate

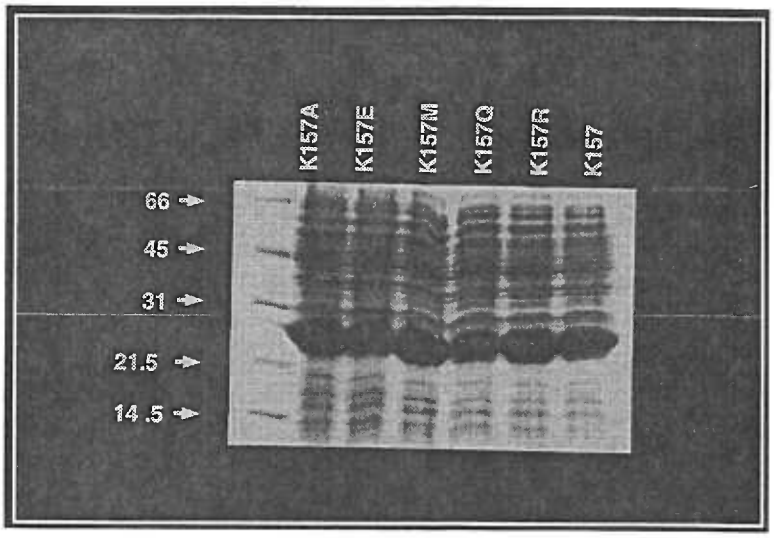

L. donovani HGPRT Purification

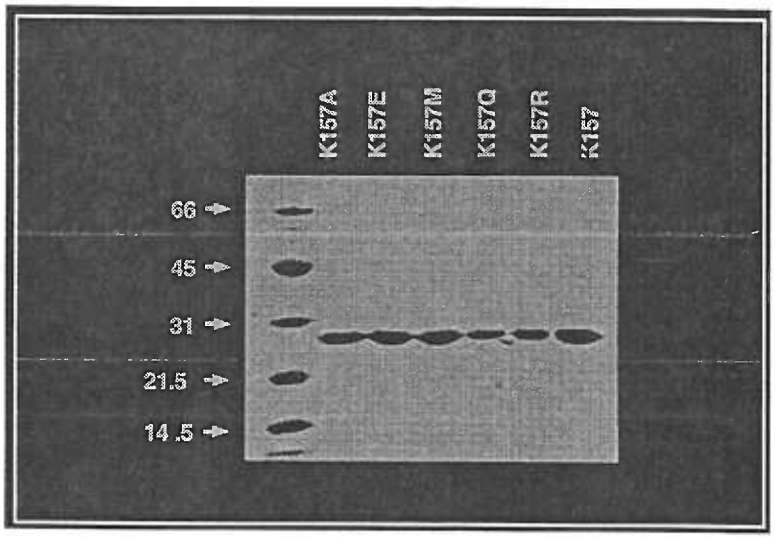

Km values for the wild type enzyme were 4.1 ± 0.5 μM for guanine and 7.8 ± 1.0 μM for hypoxanthine, which are in fairly close agreement with published values for the native enzyme (37). Five trials were completed in obtaining these values. Mutant Km values were raised between approximately 10 to 40 fold (Figure 23). PRPP kinetics were attempted, but substrate concentrations of 500 μM hypoxanthine for the mutants appeared to give rise to substrate inhibition and attempts to extrapolate the values using lower substrate concentrations were also unsuccessful because the results were too variable to obtain useful data. The wild type and mutant enzymes were also tested for activity with adenine and xanthine as substrates, but showed no APRT or XPRT activity (data not shown).

Circular dichroism studies on the wild type and all five mutants were performed to show that the observed effects were not due to the global enzyme structure being modified. These studies showed that all mutants were folded properly and similar to the wild-type enzyme in overall secondary structure (Figure 24).

Figure 23

Kinetics

The following table shows the K_m and V_{max} for the wild type and all mutants for both hypoxanthine and guanine substrates. Kinetic measurements used hypoxanthine concentrations up to a maximum of 500 µM, and guanine concentrations to a maximum of 150 µM due to solubility constraints. It also shows complementation results for hypoxanthine and guanine on growth of transformed SΦ609 cells; wild type and all mutants are represented. The large plus signs for the wild type indicate strong complementation, the small plus signs indicate weak complementation, and the minus signs indicate no complementation.

Kinetics

	Km (uM)		Vmax (umol/min/mg)		Complementation	
	Gua	Hyp	Gua	Hyp	Gua	Hyp
WT-K157	4.1±0.5	7.8±1.0	49±1	29±1	+	+
A157	146±7	105±9	14±2	13±1	-	+
E157	77±10	97±4	8.9±0.5	25±3	-	-
M157	131±12	222±17	3.7±0.4	24±3	-	-
Q157	118±8	78±9	7.6±1.0	23±2	-	-
R157	50±7	215±12	20±3	80±10	-	+

Figure 24

Circular Dichroism

Hans Peter Bachinger's lab performed the circular dichroism studies and analysis of the results showed the all enzymes were properly folded and similar to the wild type enzyme in overall secondary structure. The biggest difference is seen in the glutamic acid mutant, but the analysis of the data indicated that overall secondary structure was still intact.

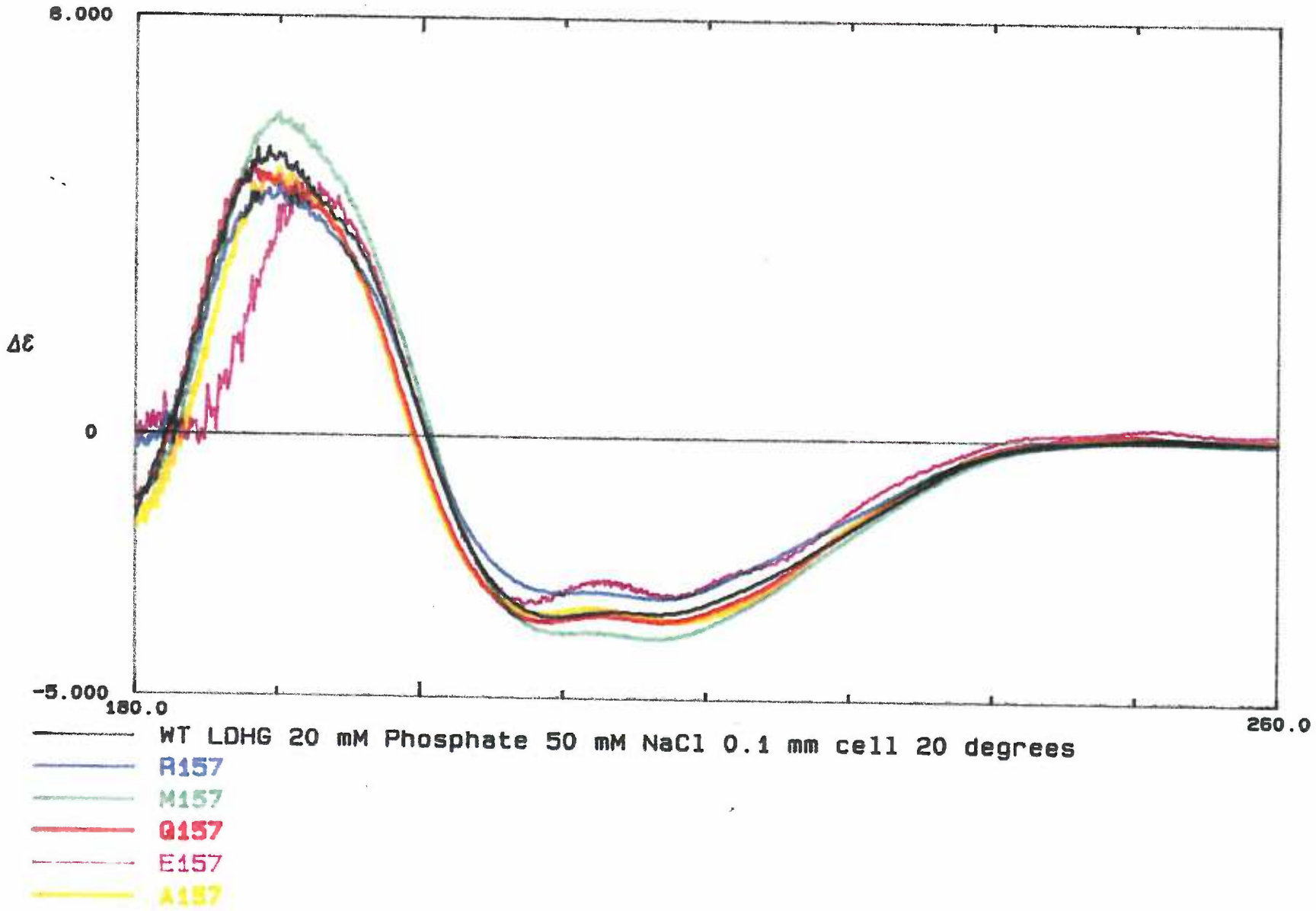
8.000
Δε
0
-5.000
180.0
260.0
WT LDHG 20 mM Phosphate 50 mM NaCl 0.1 mm cell 20 degrees
R157
M157
Q157
E157
A157

J. Discussion

While x-ray crystallographic studies would have been more revealing, site-directed mutagenesis of the of the Lys 157 residue of the *L. donovani* HGPRT has shown that this conserved Lys residue plays an important role in the functionality of the enzyme. This result is not surprising based on the structures of the HGPRT enzyme showing the hydrogen bonding role played by this conserved Lys residue (43,44,45). The *T. gondii* HGPRT structure and its analysis suggested that the Lys-157 residue in *L. donovani* HGPRT would be critical in maintaining the highly reactive orientation of the purine bases, guanine and hypoxanthine, with respect to the bound PRPP substrate (45).

It is interesting to note that the arginine mutant created the smallest Km increases with respect to guanine, but one of the highest when it came to hypoxanthine. It may be that while both guanine and hypoxanthine no longer hydrogen bond at the 6 carbonyl oxygen, the guanine may be stabilized by hydrogen bonding between its 2 amino group and adjacent residues, while this amino group

is absent in hypoxanthine. Without the O6 hydrogen bond, the hydrogen bonding of the amino group in guanine may skew its orientation thwarting catalysis. This suggestion is further supported by the ability of hypoxanthine to allow weak complementation during growth of transformed auxotrophic SΦ609 bacteria, while guanine did not show any ability to complement this mutant. It appears that the highly active orientation of both purines is no longer stabilized by bonding to the 6 carbonyl oxygen. This is supported by the catalytic model suggested by the *T. gondii* structure of Heroux, Borhani *et al.* (45), noting the position stabilizing role of this conserved lysine residue.

The differences in the Vmax between guanine and hypoxanthine are also the greatest in the arginine mutant, advancing the idea that the 2 amino group of guanine is involved in hydrogen bonding because the guanine is not able to turnover as easily in the active site as the hypoxanthine. In fact, the Vmax for hypoxanthine in the arginine mutant is higher than the wild-type enzyme, implying that its

loss of the O6 hydrogen bond enhances its ability to turnover more rapidly than even the wild type enzyme. Steric considerations, such as a potentially larger active site pocket caused by the mutation to the larger arginine may also be involved, and a larger active site may even inhibit the closing of loop II.

It should be noted that the values of Km and Vmax obtained for the arginine mutant may be in error. This type of shift was unexpected and may indicate that substrate saturation may not be achieved for this mutant. The marked change in activity does show that the Lys-157 hydrogen bond to the O6 of the purine base is important for effective catalysis.

The only other mutant that allowed hypoxanthine to weakly complement growth of the auxotrophic *E. coli* SΦ609 strain was the alanine mutant. In the case of the alanine mutation, it appears that the potential shrinking of the active site pocket based on the smaller size of alanine in comparison to lysine may have created steric hindrance, which may be responsible for the observed effects. With the

alanine mutant, the hypoxanthine had a greater Km than the guanine; this appears to be based on the larger size of the guanine with its 2 amino group creating greater steric hindrance for guanine than hypoxanthine in the active site.

Based on the *T. gondii* structure, it appears that many of the mutations might allow the purine bases to hydrogen bond in an opposite orientation. The loss of the hydrogen bond from Lys-157 to the O6 of the purine might allow the purine N7 to end up oriented toward the PRPP, instead of the N9, which would completely thwart the reaction. The complete loss of this hydrogen bond or an improperly oriented hydrogen bond in the mutants may also skew the orientation of the purine base effectively destroying catalytic activity.

Another possible effect of the mutations on enzymatic activity involves the orientation of the Phe-164 residue in the active site, in relation to the conserved tyrosine residue. As noted in the *T. gondii* structure, the close orientation of the tryptophan, its corollary to the *L. donovani* Phe-164, in relation to the conserved tyrosine residue

appears to be responsible for assisting in stabilization of the *oxocarbenium* ion intermediate in the transition state (see Figure 16). Any change in the orientation of the *L. donovani* active site Phe-164 may affect its ability to coordinate with the conserved tyrosine residue essentially removing or greatly reducing the ability of the enzyme to stabilize the *oxocarbenium* ion. Substitution of smaller or larger residues at Lys-157 may act to shift the orientation of the Phe-164 in the *L. donovani* HGPRT protein negatively affecting stabilization of the oxocarbenium ion intermediate.

In general, Vmax decreases were greater for guanine than hypoxanthine for all of the mutants. This also appears to indicate that hypoxanthine had a greater ability to turnover in the active site than guanine, supporting the suggestions that the 2 amino group of guanine allowed for hydrogen bonding in the active pocket and tended to slow turnover rates for guanine. However, when the Km was similar for guanine and hypoxanthine, the increased turnover rates for hypoxanthine versus guanine

suggested this effect may have been due to the fact that guanine is slightly larger and may not be able to enter and leave the modified active site as quickly as hypoxanthine due to its larger size because of steric constraints.

Catalytic pocket size and specific geometrical structure is critical for HGPRT, based on the compression of the substrates through the closing of loop II pulling the core and hood domains tightly together (45). Any change in the active site geometry could keep a Mg^{2+} ion from orienting correctly or possibly even keep one of the Mg^{2+} ions out of the active site diminishing catalysis.

Any mutants that might result in the expansion of the active site may also reduce the compression on the PRPP substrate and affect the ability of the enzyme to maintain the high energy, strained conformation of the PRPP that approximates the transition state. The only larger amino acid was arginine, which may have enlarged the active site and reduced PRPP substrate compression, which would likely have a strong impact on the catalytic activity of the enzyme.

Except for alanine, the mutations chosen were close in size to lysine. Glutamic acid and glutamine are slightly smaller than lysine, and with methionine gave a good range of variation in charge and polarity: methionine is mostly non-polar and hydrophobic; glutamic acid carries a negative charge, and is acidic and hydrophilic; and glutamine carries no charge, but is polar and hydrophilic. This allowed for a good contrast to lysine, which carries a positive charge, and is basic and hydrophilic. Arginine is positively charged, basic, and hydrophilic, like lysine.

The charge character of the amino acid substitutions may also play a significant role in affecting the catalytic activity of the enzyme. The *T. gondii* structure showed how critical the coordination of charges and water molecules around the PRPP were (45).

A hydrophobic substitution, such as the methionine mutant, though approximately the same size as lysine, may push water molecules around in the active site disallowing important interactions between these water molecules, Mg^{2+}, surrounding

amino acids, and PRPP, which Heroux, Borhani, *et al.* (45) showed to be so important.

A negatively charged substitution, such as the glutamic acid mutant, may tend to repel the O6 of the purine base and may also cause repulsion and reorientation of the conserved active site aspartic acid residue that appears to be in close proximity in the *T. gondii* structure (See Figure 13). This aspartic acid residue helps to stabilize the orientation of the purine base in the active site through a hydrogen bond to the N7 of the purine base; any change in orientation of this aspartic acid residue would have a negative impact on catalysis.

None of the three other amino acids, glutamine, glutamic acid, or methionine showed any ability to provide complementation to allow growth of a transformed auxotrophic bacterial strain. If any of them were able to form a hydrogen bond to the O6 of the purine base, it would suggest that the hydrogen bond skewed the orientation of the purine base creating a poor alignment with PRPP.

One final observation that was of interest was the ability to purify all of the mutants on a GTP agarose affinity column. This ability may be due to the fact that GTP was used instead of GMP, the product of the enzyme. GTP in combination with the Mg^{2+} present in the TMD buffer may have been able to bind to the PRPP binding domain of the enzyme, as the mutations affected only the purine binding site. The pyrophosphate moiety of the PRPP binds strongly to the enzyme in coordination with the Mg^{2+} ions (45) (See Figures 12 and 13). This same type of binding may be responsible for the ability to purify all of the mutants on the GTP agarose column.

K. Conclusions and Subsequent Research

Lysine 157 is involved in hydrogen bonding to the purine bases hypoxanthine and guanine as shown through crystallographic studies and suggested by the 10 to 40 fold increases in relative Km values of the mutants when compared to the wild type enzyme. While the Km is not a binding constant, its value includes the affinity of the enzyme for the substrate as well as an indication of how fast substrate is converted to the final product. Vmax values also ranged from a 2 fold decrease to a 3 fold increase. These studies clearly indicate that the role of the conserved lysine residue in bonding to the 6 carbonyl oxygen of guanine or hypoxanthine is critical for the orientation of the purine bases necessary for effective enzyme activity.

Based on subsequent research, significantly more structural and functional information on the *PRT*s has been discovered. At least 40 *PRT* crystal structures have been solved showing that the *PRT*s all exist as dimers and tetramers.(48)

A flexible loop in the structure closes over the PRPP molecule upon binding, and draws the core

and hood structures together bringing the substrates in the active site into close proximity and compressing the PRPP to approach transition state geometry (45). Prior to PRPP binding, the flexible loop is disordered (45,48).

Above the core, *PRT* proteins have a hood structure, which recognizes and binds the appropriate base through hydrogen bonding interactions, such as the bond between the conserved lysine and the 6 carbonyl oxygen of the purine base (45,48). The hood binds to the base and orients it to form a bond with the ribose phosphate moiety of the PRPP. In the case of purine PRTs, the hood is also involved in ligating the second Mg^{2+} (48).

Recently, Munagala and Wang, through site-directed mutagenesis showed the ability to change the specificity of the *T. foetus* HGXPRT into an AHGXPRT (58). Transformation to AHGXPRT was achieved by mutating the Lys-134 to a serine (58). They attribute this conversion to the ability of serine to hydrogen bond to either an amino or oxo-group, acting as a hydrogen bond acceptor for 6-

oxopurine substrates and as a hydrogen bond donor for 6-aminopurine substrates (58). In contrast to the *L. donovani* HGPRT, the T. foetus lysine to alanine mutant has some APRT activity (58).

Ongoing work in the Ullman laboratory includes work on another aspect of the purine salvage pathway—nucleoside transporters. In order for purine or pyrimidine salvage to be possible, parasites must be able to transport nucleobases across cell surface membranes. In *L. donovani*, there are two high affinity nucleoside transporters LdNT1 and LdNT2, which allow nucleosides to enter the cell to make them available to the parasite. LdNT1 transports adenosine and pyrimidine nucleosides (61), whereas LdNT2 is selective for inosine and guanosine (62). This further elucidation of the purine salvage pathway in protozoan parasites will allow targeting of both the *PRT*s and nucleoside transporters or related biochemical pathways, and is a further step toward developing better treatments for these devastating diseases.

References

1. Kuzoe F.A.S. (1993) Current situation of African trypanosomiasis. Acta Tropica 54, 153-162.

2. Englund, P.T. et al. (1995) The Replication of Kinetoplast DNA. Molecular Approaches to Parasitology 12, 147-161.

3. Molyneux, D.H. & Ashford, R.W. (1983). The Biology of Trypanasoma and *Leishmania*, Parasites of Man and Domestic Animals, Taylor and Francis, London.

4. Garcia-Zapata, M.T. & Marsden, P.D. (1992) Control of the transmission of Chagas' disease in Mambai, Goias, Brazil (1980-1988). Am. J. Trop. Med. Hyg. 46, 440-443.

5. Markel, E.K. et al. (1992) Medical Parisitology, W. B. Saunders, Philadelphia.

6. Katz, M et al. (1989) Parasitic Diseases, Springer-Verlag, New York.

7. Schmidt, G.D. & Roberts, L.S. (1989) Foundations of Parasitology, Times Mirror-Mosby, Toronto.

8. Marr, J.J. & Docampo, R. (1986) Chemotherapy for Chagas' disease: a perspective of current therapy and considerations for future research. Reviews of Infectious Diseases 8, 884-903.

9. McCabe, R.E. (1984) Mechanisms of invasion and replication of the intracellular stage in *Trypanosoma cruzi*. Infect. Immun. 46(2), 372-376.

10. Takle, G.B. & Hudson, L. (1989) Current Topics in Microbiology and Immunology 145, 81-91.

in *Trypanosoma cruzi*. Infect. Immun. 46(2), 372-376.

10. Takle, G.B. & Hudson, L. (1989) Current Topics in Microbiology and Immunology 145, 81-91.

11. James, D.M. & Gilles, H.M. (1985) Human Antiparasitic Drugs, John Wiley and Sons, New York.

12. Mihok, S. et al. (1990) Population genetics of *Trypanosoma brucei* and the epidemiology of human sleeping sickness in the Lambwe Valley, Kenya. Parasitology 100(2), 219-233.

13. Cibulskis, R.E. (1992) Genetic variation in *Trypanosoma brucei* and the epidemiology of sleeping sickness in the Lambwe Valley, Kenya. Parasitology 104(1), 99-110.

14. Wellde B.T. et al. (1989) Review of tsetse control measures taken in the Lambwe Valley in 1980-1984. Annal. Trop. Med. Parasit. 83, Supp. No. 1, 13-20.

15. Okoth, J.O. (1986) Parasitology Today 2, 88.

16. Wellde, B.T, et al. (1989) A History of Sleeping Sickness in Kenya. Annal. Trop. Med. Parasit. 83, Supp. No. 1, 1-11.

17. Okoth, JO (1991) A new approach to community participation in tsetse control in the Busoga sleeping sickness focus, Uganda. A preliminary report. Annal. Trop. Med. Parasit. 85(3), 309-314.

18. James, D.M. & Gilles H.M. (1985) Human Antiparasitic Drugs, John Wiley and Sons, New York.

19. Kreutzer, R.D. (1983) Identification of *Leishmania* spp. by multiple isozyme analysis.Am J Trop Med Hyg 32(4),703-15.

20. World Health Organization Technical Report Series (1990) 793.

21. Schmidt, G.D. & Roberts L.S. (1977) Foundations of Parasitology 72, C.V. Mosby Company, St. Louis.

22. TDR,World Health Organization (2003) Research Capacity Building in Developing Countries.

23. Ho, J.L. et al. (1992) Diminished *in vitro* production of interleukin-1 and tumor necrosis factor-alpha during acute visceral leishmaniasis and recovery after therapy. J. Infect. Disease, 165, 344-351.

24. Kaye, P.M. et al. (1991) Differential production of Th1- and Th2-derived cytokines does not determine the genetically controlled or vaccine-induced rate of cure in murine visceral leishmaniasis. J. Immunology 146(8), 2763-2770.

25. Prina, E. et al. (1990) Localization and activity of various lysosomal proteases in *Leishmania amazonensis*-infected macrophages. Infect. Immunology 58, 1730-1737.

26. Chaudhuri, G. et al. (1989) Surface acid proteinase (gp63) of *Leishmania mexicana*. A metalloenzyme capable of protecting liposome-encapsulated proteins from phagolysosomal degradation by macrophages. J. Biol. Chem. 264, 7483-7489.

27. Elias, M. et al. (1989) Bulletin of the World Health Organization 67, 43-49.

28. Guan, L.R. (1991) Bulletin of the World Health Organization 69, 595-601.

29. Chulay, J.D. et al., (1983) High-dose sodium stibogluconate treatment of

cutaneous leishmaniasis in Kenya. Trans. Royal Soc. Trop. Med. Hyg. 77, 717-721.

30. Sundar, S. et al.(2001) Resistance to treatment in Kala-azar:speciation of isolates from northeast India. Am. J.Trop. Med. Hyg. 65, 193-196.

31. Sundar, S. (2001) Drug resistance in Indian visceral leishmaniasis.Trop. Med. Int. Health 6, 849-854.

32. Sundar, S. et al. (2001) Treatment of Indian visceral leishmaniasis with single or daily infusions of low dose liposomal amphotericin B: randomised trial. Brit. Med. Jour. 323, 419-422.

33. Sundar, S. et al. (2000) Short-course of oral miltefosine for treatment of visceral leishmaniasis. Clin. Infect. Dis. 31, 1110-1113.

34. TDR,World Health Organization (2003) Drug Discovery and Development.

35. Ehrlich, P. (1909) Ber. Ddtsch. Chem. Ges. 42, 17.

36. Wigesundara S. & Woods D.D. (1962) The catabolism of cystathionine by Escherichia coli. J. Gen. Microbiol. 29, 687-702.

37. Tuttle, J.V. & Krenitsky, T.A. (1980) Purine Phosphoribosyltransferases from *Leishmania donovani*. J. Biol. Chem. 255, 909-916.

38. Glusker, J.P. & Trueblood, K.N. (1985) Crystal Structure Analysis, A Primer, Oxford University Press.

39. Martin, Y.C. (1991) Computer-assisted Rational Drug Design; Methods in Enzymology 203, 587-613.

40. Jardim, A. and Ullman, B. The Conserved Serine-Tyrosine Dipeptide in *Leishmania donovani* Hypoxanthine-Guanine Phosphoribosyltransferase is Essential for Catalytic Activity. J. Biol. Chem. 272, 8967-73 (1997).

41. Ullman, B. and Carter, D. (1997) Molecular and Biochemical Studies on the Hypoxanthine-Guanine Phosphoribosyltransferases of the Pathogenic Hemoflagellates. Int. J. Parasitol. 27, 203-213.

42. Coons, T., Hanson, S., Bitonti, A.J., McCann, P.P. and Ullman, B. (1990) Alpha-Difluoromethylornithine Resistance in *Leishmania donovani* Associated with Increased Ornithine Decarboxylase Activity. Mol. Biochem. Parasitol. 39, 77-90.

43. Eads, J.C. et al. (1994) The Crystal Structure of Human Hypoxanthine-guanine Phosphoribosyltransferase with bound GMP. Cell 78(2), 325-334.

44. Focia J.P. et al. (1998) A 1.4 Angstrom Crystal Structure for the Hyopxanthine Phosphoribosyltransferase of Trypanasoma cruzi. Biochemistry 37, 15066-15075.

45. Heroux A. et al. (2000) Substrate Deformation in a Hypoxanthine-Guanine Phosphoribosyltransferase Ternary Complex: The Structural Basis for Catalysis. Structure 8, 1309-1318.

46. Allen T.E., Hwang H.Y., Jardim A., Olafson R. & Ullman B. (1995), Cloning and expression of the hypoxanthine-guanine phosphoribosyltransferase from *Leishmania donovani*. Mol. Biochem. Parasitol. Jul 73(1-2), 133-143.

47. Mosby's Medical, Nursing & Allied Health Dictionary 4th Ed. (1994).

48. Sinha, S.C. & Smith, J.L. (2001) The PRT protein family. Current Opinion in Structural Biology 11, 733-739.

49. Arastu-Kapur, S., Ford, E., Ullman, B & Carter, NS (2003) Functional Analysis of an Inosine-Guanosine Transporter from *Leishmania donovani*. The Role of Conserved Residues, Aspartate 389 AND Arginine 393. J. Biol. Chem. 278(35), 33327-33333.

50. Aufderheide, A.C. et al., (2004) A 9,000-year record of Chagas' disease. Proc Natl Acad Sci U S A. 2004 Feb 6 [Epub ahead of print].

51. Gelb, M.H. & Hol, W.G.J. (2002) Drugs to Combat Tropical Protozoan Parasites. Science 297, 343-344.

52. Paredes R, Munoz J, Diaz I, Domingo P, Gurgui M, Clotet B. (2003) Leishmaniasis in HIV infection. J. Postgrad Med. 49, 39-49.

53. Aronov, A.M. et al., (2000) Rational Design of Selective Inhibitors of Tritchomons foetus Hypoxanthine-Guanine-Xanthine Phosphoribosyltransferase. Biochemistry 39 (16) 4684-4691.

54. Castro, J.A., Diaz de Toranzo, E.G. (1988). Toxic effects of nifurtimox and benzidazole, two drugs used against American Trypanosomiasis (Chagas' disease). Biomedical and Environmental Science 1, 19-33.

55. Blum, J. & Burri, C. (2002). Treatment of late stage sleeping sickness caused by T. b. gambiense: a new approach to the use of an old drug. Swiss Med Wkly 132, 51-56.

56. Burley, S.K. & Petsko, G.A. (1985). Aromatic-aromatic interaction: a mechanism of protein structure stabilization.

57. Ma, J.C. & Dougherty, D.A. (1997). The cation-• Interaction. Chem. Rev. 97, 1303-1324.

58. Munagala, N.R. & Wang, C.C. (1998). Altering the Purine Specificity of Hypoxanthine-Guanine-Xanthine Phosphoribosyltransferase from *Tritrichomonas foetus* by Structure-Based Point Mutations in the Enzyme Protein. Biochemistry 37, 16612-16619.

59. Berman, J.D. *et al.* (1983). Activity of Purine Analogs Against Leishmania tropica Within Human Macrophages *In Vitro.* Antimicrobial Agents and Chemotherapy 24(2), 233-236.

60. Swiss Tropical Institute Report 1999-2000.

61. Vasudevan, G., Carter, N.S., Drew, M.E., Beverley, S.M., Sanchez, M.A.,Seyfang, A.S., Ullman, B. & Landfear, S.M. (1998) Proc. Natl. Acad. Sci. USA 95, 9873-9878.

62. Carter, N.S., Drew, M.E., Sanchez, M.A., Vasudevan, G., Landfear, S.M. & Ullman, B. (2000) J. Biol. Chem. 275, 20935-20941.

63. Philips, C.L., Ullman, B., Brennan, R. & Hill, C.P. (1999). Crystal structures of adenine phosphoribosyltransferase from *Leishmania donovani*. EMBO J. 18, 3533-3545.